A Revised Diagnosis of the Blood-Feeding Candiru Genus Paravandellia (Siluriformes: Trichomycteridae: Vandelliinae) with Descriptions of Three New Species

Authors: Henschel, Elisabeth, Baskin, Jonathan N., Collins, Rupert, and Lujan, Nathan K.

Source: American Museum Novitates, 2024(4024) : 1-36

Published By: American Museum of Natural History

URL: https://doi.org/10.1206/4024.1

AMERICAN MUSEUM NOVITATES

Number 4024, 36 pp. June 28, 2024

A revised diagnosis of the blood-feeding candiru genus *Paravandellia* (Siluriformes: Trichomycteridae: Vandelliinae) with descriptions of three new species

ELISABETH HENSCHEL,[1] JONATHAN N. BASKIN,[2] RUPERT COLLINS,[3] AND NATHAN K. LUJAN[4]

ABSTRACT

The taxonomy of the blood-feeding candiru catfish genus *Paravandellia* is poorly resolved, incomplete, and hindered by a complex nomenclatural history, with many species being arbitrarily synonymized, considerable morphological and geographic variation being unevaluated, and morphological boundaries between the genus and its sister, *Paracanthopoma*, differing among authors. Herein, we describe three new species of *Paravandellia* based on photomicroscopy, cleared and stained specimens, and μCT imagery. We also reevaluate diagnostic character states for *Paravandellia* and *Paracanthopoma*, propose a new character to diagnose *Paravandellia*, and present our discovery of a possible type specimen of *Parabranchioica teaguei* and additional non-type specimens of *Branchioica bertoni*, junior synonyms of *Parav. oxyptera*. Based on these observations, we confirm *Parav. alleynei* and a recent newly described species of *Paracanthopoma* as members of a rediagnosed, putatively monophyletic *Paravandellia*, increasing its richness from two to seven species. We also discuss interrelationships of *Paravandellia* species based on the characters described.

[1] Laboratory of Molecular Systematics (BEAGLE), Department of Animal Biology, Federal University of Viçosa, Minas Gerais, Brazil; Laboratory of Systematics and Evolution of Teleost Fishes, Institute of Biology, Federal University of Rio de Janeiro.

[2] Biological Sciences Department, California State Polytechnic University, Pomona, California; Natural History Museum of Los County, Los Angeles; Department of Ichthyology, American Museum of Natural History, New York.

[3] Department of Life Sciences, Natural History Museum, London.

[4] Department of Natural History, Royal Ontario Museum, Toronto; Department of Ecology and Evolutionary Biology, University of Toronto.

 ISSN 0003-0082

INTRODUCTION

Trichomycteridae is an exclusively neotropical fish family containing 424 species commonly known as pencil catfishes, candirus, and carneros (Fricke et al., 2024). It is the second most species-rich family of catfishes (Siluriformes) and is divided into nine subfamilies: Copionodontinae (7 spp.), Glanapteryginae (15 spp.), Microcambevinae (20 spp.), Sarcoglanidinae (12 spp.), Stegophilinae (28 spp.), Trichogeninae (3 spp.), Trichomycterinae (308 spp.), Tridentinae (10 spp.), and Vandelliinae (21 spp.) (Costa et al., 2020a; Ochoa et al., 2020; Fricke et al., 2024). Whereas most trichomycterids share with other small catfishes a dietary preference for aquatic invertebrates (e.g., Alexander, 1966; Oyanedel et al., 2018), several trichomycterid taxa exhibit remarkable cranial specializations used for distinctive diets. Among these are a wide range of tooth morphologies, such as spatulate teeth for algae-scraping (Copionodontinae; Zanata and Primitivo, 2014), claw-shaped teeth for carrion-feeding (*Pareiodon microps* Kner, 1855; Baskin et al., 1980; Roberts, 1972; Fernández and Schaefer, 2009; Bonato et al., 2018), multiple rows of numerous recurved villiform teeth used for eating the mucus, scales, and skin of other fishes (Stegophilinae, Tridentinae), and medial clusters of elongate, pungent mandibular teeth for opening branchial blood vessels to consume the blood of other vertebrates (Vandelliinae; Kelley and Atz, 1964; Machado and Sazima, 1983; Zuanon and Sazima, 2003).

Given their sanguinivorous diet, species of Vandelliinae are commonly known as vampire catfishes, and their distinctive life history is associated with numerous apomorphic cranial modifications, reductions, and losses. In addition to pungent mandibular teeth, vandelliines have lateral clusters of distal, clawlike or scalpelloid premaxillary teeth, a toothed, azygous, anteromedial bone commonly referred to as the "median premaxilla" positioned between the true premaxillae, a cartilaginous fourth pharyngobranchial, and a wide and loose dentary symphysis that lack ligaments. They also lack the upper pharyngeal tooth plate, the fifth ceratobranchial, hypobranchials two and three, and the mesocoracoid (Baskin, 1973). These features, which are mostly presumed to be adaptations for host attachment and blood-feeding, support the group's monophyly (Baskin, 1973; Datovo and Bockmann, 2010; DoNascimiento, 2015). Vandelliinae monophyly is further reinforced by several multilocus and genomic datasets (Fernández and Schaefer, 2009; Ochoa et al., 2017, 2020; Costa et al., 2020a).

Vandelliinae currently contains 21 species allocated to four genera: *Paracanthopoma* Giltay, 1935 (13 spp.), *Paravandellia* Miranda-Ribeiro, 1912 (2 spp.), *Plectrochilus* Miranda Ribeiro, 1917 (3 spp.), and *Vandellia* Valenciennes, 1846 (3 spp.; Fricke et al., 2024). The subfamily is broadly distributed across lowlands of northern cis- and trans-Andean South America, including the Amazon, Orinoco, Essequibo, Cauca-Magdalena, Araguaia-Tocantins, and Paraná-Paraguay drainage basins, where they are most commonly collected either from the bodies of host fishes on which they were feeding prior to capture, or in sandbanks where they often remain shallowly buried when not feeding (Miranda-Ribeiro, 1912; Eigenmann, 1917; Di Caporiacco, 1935; Giltay, 1935; Miles, 1943; Dagosta and de Pinna, 2021; Henschel et al., 2021a, 2021b; de Pinna and Dagosta, 2022). Within the Vandelliinae's distinctive dietary niche, the subfamily has diversified in body size, spanning a 13× range from smallest to largest, from species of *Paracanthopoma* that reach a maximum known size of only 1.5 cm standard length

(SL) (de Pinna and Dagosta, 2022), to some species of *Vandellia* that reach up to 20 cm SL (de Pinna and Wosiacki, 2003).

Baskin (1973) provided the first cladistic analysis of Vandelliinae, proposing a sister relationship between *Vandellia* and *Plectrochilus*, a clade that was also supported by subsequent morphology-based studies by Schmidt (1993) and DoNascimiento (2012) and the molecular analysis of Fernández and Schaefer (2009). In contrast, relationships and taxonomic boundaries of *Paravandellia* and *Paracanthopoma* have varied across studies. Specimens of *Paracanthopoma* were not available to Baskin (1973), yet the author considered this genus to be sister to all other vandelliines based on the presence of a free branchiostegal membrane across the isthmus, the plesiomorphic condition for Trichomycteridae (Baskin, 1973). Later, in the first cladistic analysis focused exclusively on Vandelliinae, Schmidt (1993) found *Paravandellia* to be sister to all other genera, with *Paracanthopoma* being sister to *Vandellia* + *Plectrochilus*. This last clade (*Paracanthopoma* + (*Plectrochilus* + *Vandellia*)) was supported by the shared, derived absence of medial teeth on the premaxilla, presence of a medially forked premaxilla, distal margins of the mesethmoid forked, fewer dentary teeth, and interopercular odontodes posteriorly oriented. Schmidt (1993) also considered the presence of medial teeth on the premaxilla and greater than six dentary teeth to be synapomorphies of *Paravandellia*, and he considered the free branchiostegal membrane across the isthmus (treated as a reversal), an enlarged axillary gland, and a medial, azygous supratemporal lateral-line pore (= single s6 pore at juncture of fused epiphyseal branches) also to be synapomorphies of *Paracanthopoma*. Subsequently, in a cladistic analysis for his unpublished Ph.D. dissertation, DoNascimiento (2012) proposed that *Paracanthopoma* and *Paravandellia* form a clade sister to *Vandellia* + *Plectrochilus.* The author suggested several synapomorphies for *Paracanthopoma*, such as epioccipital fused with gasbladder capsule, restricted articulation between parietosupraoccipital and first vertebra, coronoid process of retroanguloarticular continuous with dorsal mandibular margin, dorsal process on proximal margin of premaxilla connected to autopalatine, absence of fourth epibranchial, and several other characters related to dorsal- and anal-fin basal radials. For DoNascimiento (2012), the azygous s6 pore is exclusive to *Parac. parva* Giltay, 1935, and the free branchiostegal membrane across the isthmus (= "velum" of Dagosta and de Pinna, 2021) is an "informative homoplasy" for the genus (i.e., useful for diagnosis, but not a synapomorphy). Regarding the definition of *Paravandellia*, DoNascimiento (2012) proposed two synapomorphies: pterosphenoid laterally expanded, and articulation of the hyomandibula with the neurocranium restricted to the sphenotic. DoNascimiento (2012) also regarded the presence of medial teeth on the premaxilla as informative for diagnosing *Paravandellia*, but not a synapomorphy. Nine years later and without illustration, Dagosta and de Pinna (2021) proposed the following as exclusive character states of *Paracanthopoma*: presence of a free branchiostegal membrane across the isthmus, a distally forked maxilla, and bilateral dorsal flanges on the median premaxilla. In the same work, the authors state that the free branchial membrane seen in *Paracanthopoma* is a neomorphic structure, which they call the "branchiostegal velum," stating that it is probably derived from the branchiostegal membrane. However, absence of a cladistic analysis and anatomical illustrations hinders the interpretation, critique, and acceptance of this new term and hypothesis.

The next year, de Pinna and Dagosta (2022) described nine new species of *Paracanthopoma* and discussed the monophyly, synapomorphies, and external relationships of the putative clade formed by *Paracanthopoma* + *Paravandellia* in light of the cladistic analysis of DoNascimiento (2012). de Pinna and Dagosta (2022) diagnosed *Paracanthopoma* based on nine putative synapomorphies: (1) presence of a "branchiostegal velum" [= free branchiostegal membrane of Baskin (1973), Schmidt (1993) and DoNascimiento (2012)]; (2) median premaxilla with bilateral dorsal flanges; (3) median premaxilla with well-defined median posterior recess; (4) maxilla distally forked; (5) posterior articular process of autopalatine oriented parallel to neurocranium; (6) premaxilla with deep indentation on anterior margin; (7) coronoid process formed mainly by dentary process; (8) absence of upper pharyngeal toothplate; and (9) restricted joint between parietosupraoccipital and neural arch of complex vertebra. De Pinna and Dagosta (2022) also proposed nine synapomorphies for *Paravandellia*: (1) maxilla greatly expanded; (2) mesethmoid with anterior margin having small notch delimited by bilateral flanges; (3) mandibular coronoid process formed mainly by retroangular; (4) orbitosphenoid with narrow ventral arm; (5) ventral arm of orbitosphenoid and anteroventral portion of sphenotic-prootic-pterosphenoid distant; (6) opercle with dorsal process lacking flange; (7) opercle with bony expansion lateral to articulation with hyomandibula; (8) urohyal with widely spaced anterior process; and (9) fourth ceratobranchial missing or entirely cartilaginous. For these authors, the presence of medial teeth on the premaxilla, regarded as exclusive to *Paravandellia* by Schmidt (1993) and Henschel et al. (2021a), is "likely" a plesiomorphic condition for Trichomycteridae, thus neither exclusive nor diagnostic of *Paravandellia*, being present also in two species of *Paracanthopoma* (de Pinna and Dagosta, 2022: 83).

De Pinna and Dagosta (2022) also changed the generic composition of *Paravandellia*, moving *Paravandellia alleynei* Henschel et al., 2021, to *Paracanthopoma* based on the new generic diagnoses summarized above. Currently, *Paracanthopoma* comprises 13 species: *Parac. parva* Giltay, 1935, *Parac. saci* Dagosta and de Pinna, 2021, *Parac. cangussu* Henschel, Katz and Costa, 2021, *Parac. alleynei*, *Parac. ahriman* de Pinna and Dagosta, 2022, *Parac. capeta* de Pinna and Dagosta, 2022, *Parac. carrapata* de Pinna and Dagosta, 2022, *Parac. daemon* de Pinna and Dagosta, 2022, *Parac. irritans* de Pinna and Dagosta, 2022, *Parac. malevola* de Pinna and Dagosta, 2022, *Parac. satanica* de Pinna and Dagosta, 2022, *Parac. truculenta* de Pinna and Dagosta, 2022, and *Parac. vampyra* de Pinna and Dagosta, 2022. In aggregate, these species are distributed throughout lowland rivers draining the Guiana and Brazilian Shield highlands (Henschel et al., 2021a; de Pinna and Dagosta, 2022). Conversely, de Pinna and Dagosta (2022) left *Paravandellia* with only two long-recognized species, *Parav. oxyptera* Miranda Ribeiro, 1912, and *Parav. phaneronema* (Miles, 1942), in a spectacularly disjunct geographical distribution, with the former restricted to the Paraná-Paraguay and Uruguay River basins south of the Amazon and the latter to the Cauca-Magdalena River basin west of the Andes and northwest of the Amazon (de Pinna and Wosiacki, 2003; Henschel et al., 2021a, 2021b). No valid species of *Paravandellia* are currently recognized from throughout the vast Amazon, Orinoco, or Essequibo river basins.

The recent flurry of taxonomic work on *Paracanthopoma*, including a redescription of the type species *Parac. parva* based on high-resolution X-ray CT imagery of the holotype (Hen-

schel et al., 2021b), has significantly improved our understanding of taxonomic diversity in this genus. By comparison, taxonomic progress on *Paravandellia* remains hindered by an overall scarcity of material, limited access to type specimens, a complicated nomenclatural history, and ambiguity regarding its diagnosis. *Paravandellia oxyptera* Miranda Ribeiro, 1912, type species of the genus, was described based on a single specimen collected from aquatic lettuce roots in the upper Paraguay River basin (Miranda Ribeiro, 1912). Eigenmann (1917) described *Branchioica*, diagnosing it in part by the presence of small medial teeth on the premaxilla, and suggesting that it might be a junior synonym of *Paravandellia* given its origin in the lower Paraguay River (Eigenmann, 1917: 702). The very next year, *Pleurophysus* Miranda Ribeiro, 1918, was described based on five specimens from the Claro River, a tributary of the Paranaíba River more than 1000 km from the type locality of *Parav. oxyptera* (Miranda Ribeiro, 1918). Twenty-one years later, Devincenzi and Vaz-Ferreira (1939) described *Parabranchioica* , 1939, a genus that was also diagnosed by the presence of small teeth lateral to the median premaxilla (i.e., medial teeth on the premaxilla; Devincenzi and Vaz Ferreira, 1939). De Pinna and Wosiacki's checklist (2003) considered *Branchioica*, *Pleurophysus*, and *Parabranchoica* as junior synonyms of *Paravandellia*, which was consistent with prior hypotheses (e.g., Eigenmann, 1917) but still unsupported by published evidence. They also considered the types of *Parabranchioica teaguei* DeVincenzi and Vaz Ferreira, 1939, the type species of *Parabranchioica*, to be unknown (de Pinna and Wosiacki, 2003).

This study is motivated in part by the likely underestimation of *Paravandellia* taxonomic diversity, given that specimens assignable to this genus have for decades been collected throughout the vast Amazon, Orinoco, and Essequibo drainages where no valid species are currently recognized (E.H., N.K.L. personal obs.). Indeed, μCT-imagery that we generated from seven such specimens from the upper Orinoco and western and central Amazon, combined with comparative μCT-imagery of topotypes for both nominal species, revealed morphological variation sufficient to justify our conservative recognition of three additional species as new to science. Additionally, we reevaluate the morphological diagnoses, taxonomic composition and boundaries of both *Paravandellia* and *Paracanthopoma* based on our observations of considerable intergeneric variation and overlap in various characters recently proposed as diagnostic for each genus. Finally, we report the results of an extensive search of the Ichthyological Collection of the Natural History Museum, London, by two of us (J.N.B. and R.C.), which revealed a possible type specimen of *Parabranchoica teaguei* and additional nontype specimens of *Branchioica bertoni* Eigenmann, 1917, allowing these specimens to be μCT-scanned and finally compared in detail with other putative conspecifics.

MATERIAL AND METHODS

Specimen Collection and Curation

Specimen collections were made in Brazil with a permit provided by Instituto Chico Mendes de Conservação da Biodiversidade as approved by Instituto Chico Mendes de Conservação da

Biodiversidade (ICMBio; permit number 54636-3), in Ecuador with a permit provided by the Ministerio del Ambient, Agua y Transición Ecológico (permit number MAAE-DBI-CM-2021-0161), and in Venezuela with a permit provided by the Ministerio de Poder Popular para la Agricultura y Tierras – Instituto Socialista de la Pesca y Acuicultura (permits 2005-000014 and 2010-223137 to N.K.L.). Specimens were collected with combinations of either dip nets, 2 × 3 m, 3 mm (straight) mesh seines, or a backpack electrofisher, and immediately euthanized in either a buffered solution of ethyl-3-amino-benzoat-methansulfonate (MS-222) at a concentration of 250 mg/l or a 0.08% solution of eugenol (clove oil) and water until entirely ceasing opercular movements for at least 30 min, according to national animal welfare laws and guidelines approved by either CEUA-CCS-UFRJ (Ethics Committee for Animal Use of Federal University of Rio de Janeiro; permit number: 065/18) or the Royal Ontario Museum Animal Use Committee (protocol number 2021-004). Other material examined in this study were historic, formalin-fixed, ethanol-preserved specimens from museum collections. CT-imagery and morphological characters were obtained from fixed, preserved specimens deposited in either the American Museum of Natural History in New York (AMNH), the Academy of Natural Sciences of Drexel University in Philadelphia (ANSP), the Auburn University Museum of Natural History in Auburn, Alabama (AUM), the Pontifícia Universidade Católica do Rio Grande do Sul, Museu de Ciências e Tecnologia, Rio Grande do Sul, Porto Alegre, Brazil (MCP), the Royal Ontario Museum in Toronto, Canada (ROM), the Ichthyological Collection of the Instituto de Biologia, Universidade Federal do Rio de Janeiro, Rio de Janeiro (UFRJ), the Natural History Museum, London (BMNH), or the Smithsonian Institution National Museum of Natural History in Washington, DC (USNM). Comparative material is listed in Supporting Information File S1.

Imaging and Analysis

Measurements and counts follow Costa (1992), with modifications proposed by Costa et al. (2020b). Measurements are presented as percentages of standard length (SL), except for subunits of the head, which are expressed as percentages of head length (HL). Photomicrographs were taken using a Keyence VHX-6000 digital microscope (Keyence Inc., Osaka, Japan). Measurements based on photographs of fixed specimens were taken using the software ImageJ (Abràmoff et al., 2004). Specimens for osteological examination were either cleared and double-stained following Taylor and Van Dyke (1985) or μCT-scanned at varying resolutions (1.9–7.3 μm) using either a GE v|tome|x s240 dual tube 240/180 kV system (General Electric, Fairfield, CT) or a Bruker Skyscan 1173 high-energy micro-CT (Bruker Inc, Billerica, MA). CT data were edited, segmented, and colorized using VGStudio Max (v3.3–v2023.3; Volume Graphics, Heidelberg, Germany).

Anatomical Accounts

Osteological nomenclature follows Datovo and Bockmann (2010) in general, although selected terms as proposed and defined by de Pinna and Dagosta (2022) are used: **epiodonteal**

velum, **hypodontal pad**, **labial bursa**, **periodontal fold**, **scalpelloid teeth**, and **dentary lobe**. Three terms proposed by de Pinna and Dagosta (2022) that we do not use are: **branchiostegal velum**—justification for this term as a neomorph requires further examination of its evolutionary and ontogenetic relationship with the branchiostegal membrane; **dentary diastema**—this term was proposed by them for the space between the "dentary lobes," however, this term is equivalent to dentary symphysis, which is already widely used and accepted as the point or space where dentary bones meet (e.g., Baskin, 1973; Datovo and Bockmann, 2010; Dagosta and de Pinna, 2021; Henschel et al., 2021a, 2021b); and **odontodophore**—originally proposed to refer to the odontodes and associated modified soft structures of either the opercle or interopercle; however, the scope and associated modified soft structures were not precisely specified, stating only: "including both the odontodes themselves plus the associated modified soft tissues" (de Pinna and Dagosta, 2022: 3).

Vertebral counts exclude the Weberian apparatus and count the compound caudal centrum (PU1 + U1) as a single element. Caudal skeleton terminology follows Lundberg and Baskin (1969). Terminology for fin-ray counts follows Bockmann and Sazima (2004), where anterior unbranched and unsegmented rays are represented by lower-case Roman numerals, unbranched segmented rays by upper-case Roman numerals, and branched segmented rays by Arabic numerals. Branchiostegal rays are considered from medial- to lateralmost and numbered accordingly from 1 to 4.

In diagnoses, total principal fin-ray counts include only segmented rays. Abbreviations: **alc,** alcohol specimen; **cs,** cleared and stained specimen; **ct,** computed-tomography-scanned specimen; **lp,** specimen photographed alive; **pm,** specimen of which a photomicroscopic image was made.

RESULTS

Taxonomic Accounts

***Paravandellia oscarleoni*,** new species

Figures 1–3, 4D, 6D, table 1

Zoobank registration: urn:lsid:zoobank.org:act:1CDC4E66-BE89-4A9D-AFDF-0DB6A3F35C1C

Holotype: AUM 57772, 16.7 mm SL, alc, ct, pm, Venezuela, Amazonas State, 11.8 km WNW of La Esmeralda, Caño Soromoni, Ventuari-Orinoco drainage basin, 3.1938° -65.65197°, ca. 124 m above sea level, NK Lujan, M Arce, TE Wesley, EL Richmond, MB Grant, 25 March 2005, field number VEN05-39.

Paratypes: Five specimens, all Venezuela, Amazonas State, Orinoco-Ventuari drainage basin: AMNH 230907, 1, 17.4 mm SL, alc, ct, pm, Corocoro River at Corocoro Falls ca. 30 minutes upstream of Campamento Yutaje, Yutaje–Manapiare drainage basin, 5.624119° -66.123°, ca. 125 m above sea level, S.A. Schaefer, F. Provenzano, A. Rojas, 27 April 1999, field number SAS-99-05. AUM 56700, 1, 18.6 mm SL, alc, ct, 105.5 km E of San Fernando de Ata-

FIGURE 1. Holotype of *Paravandellia oscarleoni*, AUM 57772, 16.7 mm SL, Venezuela, Amazonas State, 11.8 km WNW of La Esmeralda, Caño Soromoni, Ventuari-Orinoco drainage basin, 3.1938°, -65.65197°, ca. 124 m above sea level, N.K. Lujan, M. Arce, T.E. Wesley, E.L. Richmond, M.B. Grant, 25 March 2005.

bapo, Guapuche River, first rapids ca. 20 min by boat upstream from mouth, 4.13022° -66.75379°, ca. 102 m above sea level, N.K. Lujan, M. Arce, T.E. Wesley, E.L. Richmond, M.B. Grant, 2 April 2005, field number VEN05-48. AUM 57772, 2: 1, 13.5 mm SL, alc, 1, 12.5 mm SL, cs, same data as holotype. ROM 112353, 1 alc, 17.8 mm SL, same data as holotype.

Diagnosis: *Paravandellia oscarleoni* differs from all congeners by having a broadly convex hook-shaped flange extending anteriorly from the parietosupraoccipital into the cranial fontanel (fig. 4D; vs. concave anterior margin of the parietosupraoccipital); fewer teeth on median premaxilla (fig. 5D; 10 vs. 11 in *Parav. alleynei* and *Parav. vampyra*, 13–18 in *Parav. oxyptera*, 15 in *Parav. phaneronema*, 20 in *Parav. luna* and 21–22 in *Parav. brooksi*); and by having a slightly forked distal margin of maxilla (fig. 6D; vs. completely forked in *Parav. alleynei* and *Parav. vampyra*, and blunt in *Parav. oxyptera*, *Parav. phaneronema*, *Parav. brooksi*, and *Parav. luna*). It differs from all congeners except *Parav. vampyra* and *Parav. alleynei* by having a free branchiostegal membrane across the isthmus (fig. 1; vs. fused); fewer medial teeth on premaxilla (fig. 5D; 2 vs. 3–6 in *Parav. luna*, 4–8 in *Parav. brooksi*, and 5 in *Parav. oxyptera* and *Parav. phaneronema*); more scalpelloid teeth (fig. 5D; 4 vs. 2 or 3 in *Parav. oxyptera* and *Parav*. *brooksi*, and 2 in *Parav. phaneronema* and *Parav*. *luna*); posteriorly directed opercular odontodes (fig. 6D; vs. dorsally directed); an anterior osseous flange on the ascending process of opercle (fig. 6D; vs. absence); and median premaxilla as wide as long (fig. 5D, vs. wider than long); and by lacking an anteromedial notch on the mesethmoid (fig. 4D; vs. presence). *Paravandellia oscarleoni* differs from all congeners except *Parav. vampyra* by having fewer opercular odontodes (fig. 6D; 11–15 vs. 16–17 in *Parav. alleynei*, 22–26 in *Parav. oxyptera*, 23–26 in *Parav. phanero-*

FIGURE 2. Paratype of *Paravandellia oscarleoni*, AUM 56700, 18.6 mm SL, 105.5 km E of San Fernando de Atabapo, Guapuche River, first rapids ca. 20 min by boat upstream from mouth, 4.13022°, -66.75379°, ca. 102 m above sea level, N.K. Lujan, M. Arce, T.E. Wesley, E.L. Richmond, M.B. Grant, 2 April 2005.

nema, 24–30 in *Parav. brooksi*, and 26–29 in *Parav. luna*); by having first anal-fin pterygiophore at vertical anterior to haemal spine of 22nd vertebra (vs. 23rd in *Parav. alleynei*, 24th–25th in *Parav. phaneronema*, 26th in *Parav. oxyptera*, 27th in *Parav. brooksi* and 29th–30th in *Parav. luna*). It is further distinguished from all congeners except *Parav. alleynei* by having fewer vertebrae (38–39 vs. 40–42 in *Parav. vampyra*, 42 in *Parav. brooksi*, 43 in *Parav. phaneronema*, and 44–46 in *Parav. oxyptera* and *Parav. luna*). *Paravandellia oscarleoni* differs from all congeners except *Parav. alleynei* and *Parav. phaneronema* by having median premaxilla connected to mesethmoid main axis via bilateral dorsal flanges (fig. 4D; vs. dorsal flanges absent); and differs from all congeners except *Parav. phaneronema* by having two dentary teeth (fig. 5D; vs. 4 in *Parav. alleynei* and *Parav. luna*, 4 or 5 in *Parav. brooksi*, and 5 or 6 in *Parav. oxyptera*); and differs from *Parav. oxyptera*, *Parav. phaneronema* and *Parav. brooksi* by having a total of nine principal dorsal-fin rays (vs. eight in *Parav. oxyptera* and *Parav. phaneronema*, and 11 in *Parav. brooksi*). *Paravandellia oscarleoni* is further distinguished from *Parav. alleynei* by median premaxilla being wider than long (fig. 4D; vs. longer than wide); parasphenoid being 3× longer than wide (vs. 2× longer than wide); and by lacking an anteromedial process on autopalatine (vs. presence).

Description: Morphometric data for holotype presented in table 1.

Gross external morphology: Dorsal profile of body convex from tip of snout to dorsal-fin base; approximately straight from that point to insertion of caudal-fin procurrent rays; slightly convex from that point to base of caudal fin. Ventral body profile approximately concave from mouth to ventral insertion of anal fin; approximately straight from that point to

FIGURE 3. Paratype of *Paravandellia oscarleoni*, AMNH 230907, 17.4 mm SL, Corocoro River at Corocoro falls ca. 30 minutes upstream of Campamento Yutaje, Yutaje-Manapiare drainage basin, 5.624119°, -66.121933°, ca. 125 m above sea level, S.A. Schaefer, F. Provenzano, A. Rojas, 27 April 1999.

caudal-fin insertion. Cross section of body in trunk region approximately oval, becoming gradually more compressed to dorsal-fin base. Caudal peduncle strongly compressed. Axillary gland well developed in some individuals, with conspicuous pore.

Head straight and depressed, approximately triangular in dorsal view. Eye large, with thin translucent skin covering. Anterior nostril small, covered by thin, fleshy flap. Posterior nostril located approximately midway between anterior nostril and anterior orbital rim, surrounded by fleshy flap on anterior margin. Mouth ventral, M-shaped. Nasal barbel absent. Maxillary barbel well developed, reaching posterior margin of eye. Rictal barbel vestigial. Branchiostegal membrane posteriorly continuous and free from isthmus, with a median notch in one specimen (AUM 56700).

Skull morphology: Anterior margin of mesethmoid straight. Mesethmoid cornua oriented at 45° angle to sagittal axis. Cranial fontanel triangular, occupying approximately 75% of skull roof area; delimited anteriorly by mesethmoid and frontal and posteriorly by sphenotic-prootic-pterosphenoid and parietosupraoccipital. Sesamoid supraorbital and antorbital absent. Autopalatine wide, trapezoidal, with proximal process long and parallel to sagittal axis of head, connected to lateral ethmoid. Autopalatine fenestra wide, occupying approximately 80% of autopalatine area in dorsal view. Sphenotic, prootic, and pterosphenotic robust and entirely fused. Median premaxilla scalene trapezoid, with paired bilateral flanges contacting mesethmoid main axis. Ten median premaxillary teeth arranged in two rows, anterior row with six teeth, inner row with four. Parasphenoid straight and laminar, approximately hexagonal. Anterior portion of Weberian complex fused to basioccipital-exoccipital. Weberian capsule with constricted opening at lateral

Table 1. Morphometric data for holotype and paratypes (n = 3) of *Paravandellia oscarleoni*.

	Holotype	Min	Max	Mean
Standard Length	16.7	16.1	18.2	17.0
Body Depth	15.6	9.3	15.6	12.5
Caudal Peduncle Depth	7.2	5.6	8.2	7.0
Body Width	10.2	6.2	11.5	9.3
Caudal Peduncle Width	1.8	1.8	2.5	2.2
Predorsal Length	70.1	70.1	73.3	72.0
Preanal Length	74.3	73.3	74.3	73.7
Prepelvic Length	62.9	62.9	68.3	65.0
Dorsal-fin base length	8.4	7.1	8.4	7.7
Anal-fin base length	10.2	10.2	10.6	10.4
Pectoral-fin length	12.0	8.7	14.3	11.7
Pelvic-fin length	9.0	4.3	9.0	7.0
Head Length	44.0	15.0	18.7	16.8
Head Depth	96.0	33.3	44.0	37.5
Head Width	44.0	70.4	96.0	80.0
Preorbital Length	28.0	40.7	44.0	42.0
Interorbital Width	20.0	7.4	28.0	16.7
Eye Diameter	28.0	18.5	20.6	19.7
Mouth Width	20.0	18.5	35.3	27.3
Interopercular Patch Length	36.0	7.4	20.0	14.0
Opercular Patch Length	44.0	14.8	36.0	25.8

end of long, necklike collar. Proximal end of premaxilla forked, with ventral and dorsal processes contacting anterior margin of autopalatine. Premaxilla with two medial teeth and four distal scalpelloid teeth. Maxilla thin and short, distal margin approximately straight, with anterior margin curved at 90° angle to sagittal plane and approximately 50% as long as premaxilla. Dentary with two thin, elongate, medially curved teeth arranged in single distal patch.

Opercular suspensorium: Metapterygoid small, compact, approximately cylindrical. Hyomandibula thin, with conspicuous anteromedial osseous flange; connected to sphenotic-prootic-pterosphenoid. Anterior process of hyomandibula reaching 80% of quadrate length. Preopercle long, narrow, approximately rectangular, with short anterior process reaching 40% of quadrate length. Opercular patch of odontodes wide, elliptical, located laterally on head; opercular odontodes 11–15, arranged in three irregular rows. Opercle with well-developed dorsally directed ascending process with conspicuous osseous flange, about as long as opercular patch of odontodes. Interopercular patch of odontodes narrow; interopercular odontodes 9–11.

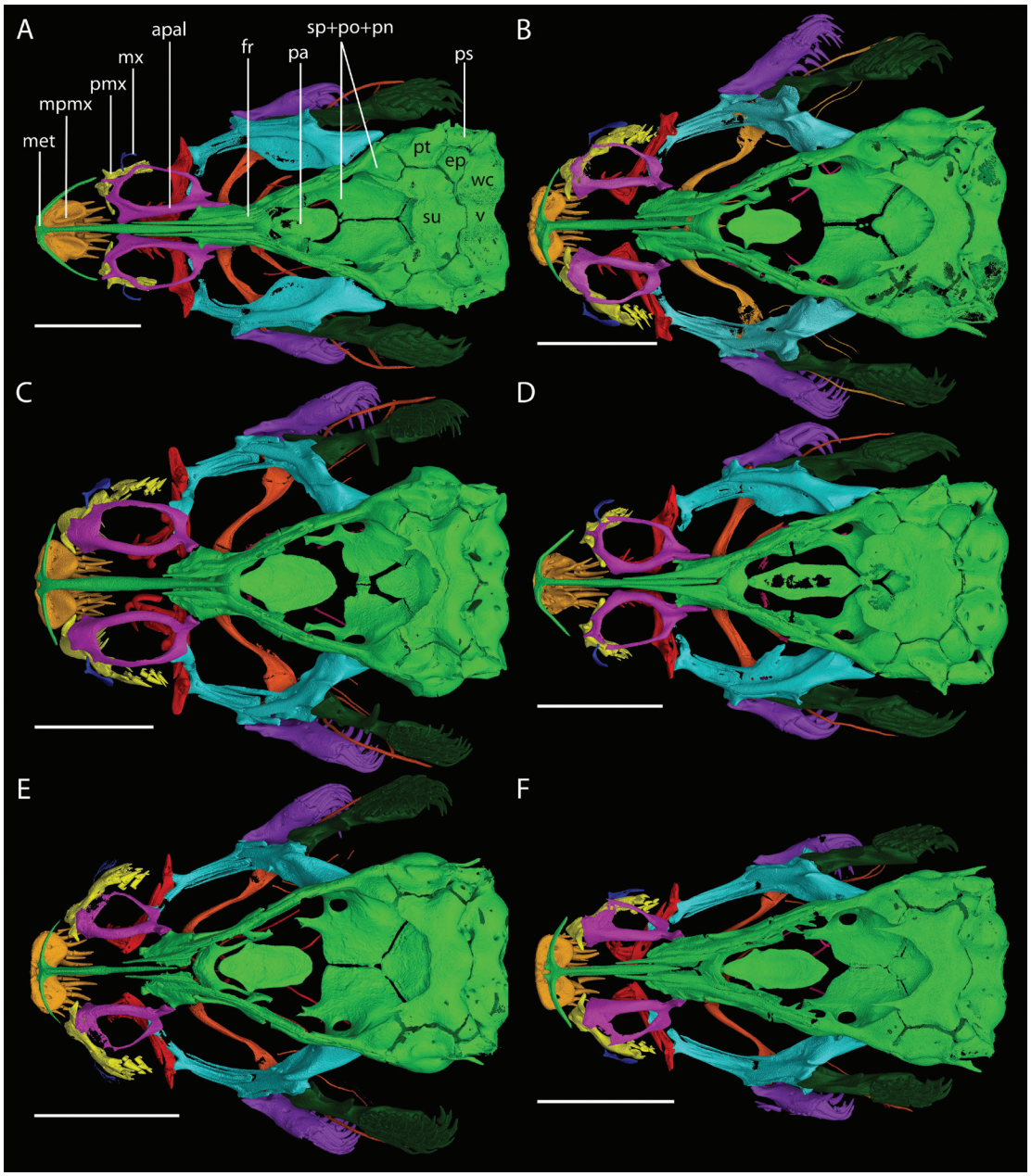

FIGURE 4. Dorsal view of skulls of **A,** *Paravandellia alleynei*, AMNH 72898, 26 mm SL; **B,** *Parav. oxyptera*, MCP 46576, ca. 20 mm SL; **C,** *Parav. phaneronema*, ROM 112356, ca. 20 mm SL; **D,** *Parav. oscarleoni*, AUM 56700, 18.6 mm SL; **E,** *Parav. brooksi*, AUM 43316 , 19.2 mm SL; **F,** *Parav. luna*, ANSP 189307, 23.8 mm SL. Abbreviations: **apal,** autopalatine; **ep,** epiotic; **fr**, frontal; **met,** mesethmoid; **mpmx,** median premaxlla; **mx**, maxilla; **pa,** parasphenoid; **pmx,** premaxilla; **pt,** pterotic; **ps,** posttemporosupracleithrum; **sp+po+pn,** sphenotic-prootic-pterosphenoid complex bone; **su,** supraoccipital; **v,** first vertebra attached to Weberian capsule; **wc,** Weberian capsule. Scale bars = 1 mm.

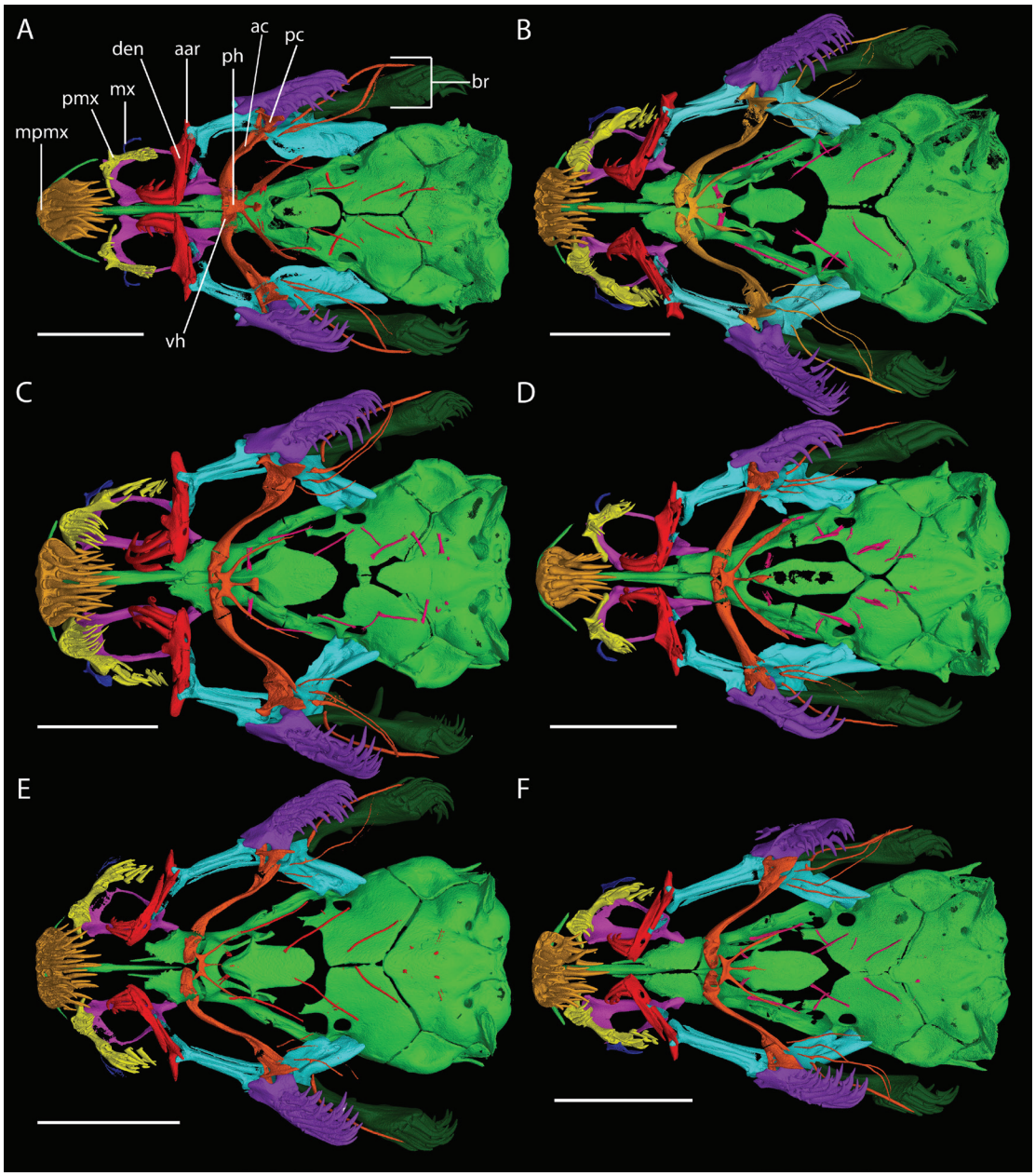

FIGURE 5. Ventral view of skulls of **A,** *Paravandellia alleynei*, AMNH 72898, 26.0 mm SL; **B,** *Parav. oxyptera*, MCP 46576, ca. 20.0 mm SL; **C,** *Parav. phaneronema*, ROM 112356, ca. 20.0 mm SL; **D,** *Parav. oscarleoni*, AUM 56700, 18.6 mm SL; **E,** *Parav. brooksi*, AUM 43316, 19.2 mm SL; **F,** *Parav. luna*, ANSP 189307, 23.8 mm SL. Abbreviations: **aar,** angulo-articular; **ac,** anterior ceratohyal; **br,** branchiostegal rays; **den,** dentary; **mx,** maxilla; **mpmx,** median premaxilla; **pc,** posterior ceratohyal; **ph,** parurohyal; **pmx,** premaxilla; **vh,** ventral hypohyal. Scale bars = 1 mm.

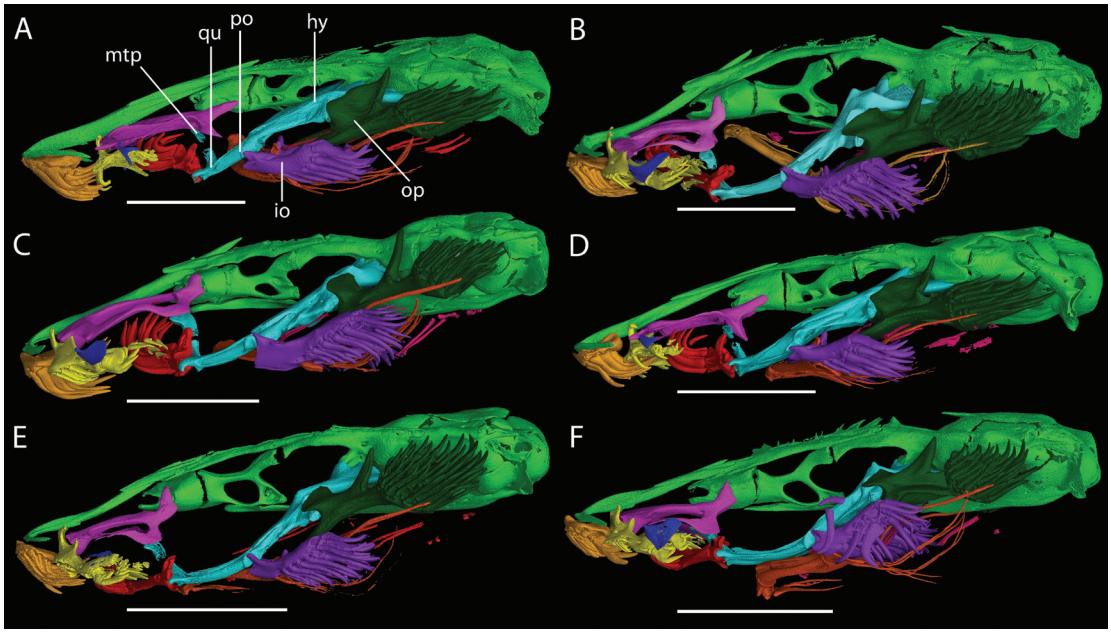

FIGURE 6. Lateral view of skull of **A,** *Paravandellia alleynei*, AMNH 72898, 26.0 mm SL; **B,** *Parav. oxyptera*, MCP 46576, ca. 20.0 mm SL; **C,** *Parav. phaneronema*, ROM 112356, ca. 20.0 mm SL; **D,** *Parav. oscarleoni*, AUM 56700, 18.6 mm SL; **E,** *Parav. brooksi*, AUM 43316, 19.2 mm SL; **F,** *Parav. luna*, ANSP 189307, 23.8 mm SL. Abbreviations: **hy,** hyomandibula; **io,** interopercle; **mtp,** metapterygoid; **op,** opercle; **po,** preopercle; **qu,** quadrate. Scale bars = 1 mm.

Opercular and interopercular odontodes thin, conical, with straight base, gradually compressed distally, with tips curved dorsomedially.

Hyoid arch: Four branchiostegal rays, all articulated with posterior ceratohyal; lateralmost branchiostegal ray (ray 4) longest, extending posterodorsally along lateral face of opercle (fig. 6D) and medial to the interopercle; remaining three medial branchiostegals curved posterodorsally ventral to opercle. Hyoid arch with thin ventral parurohyal with concave anterior margin. Anterolateral processes of parurohyal articulated with posteroventral concavity of ventral hypohyal. Posterolateral processes of parurohyal long, distally expanded, reaching articulation of anterior and posterior ceratohyal. Posteromedial process reaching half of anterior ceratohyal length with expanded tip, spoon shaped. Elongate anterior ceratohyal; short posterior ceratohyal. Dorsal hypohyal and interhyal absent.

Axial skeleton: Pectoral-fin rays I,5. Pelvic-fin rays I,5. Dorsal-fin rays iii,I,8 or 9; fin origin posterior to body midpoint; first pterygiophore immediately anterior to 21st vertebra neural spine. Anal-fin rays ii,II,5 or iii,II,6; fin origin at vertical through origin of first or second branched dorsal-fin ray; first anal-fin pterygiophore inserting immediately anterior to 22nd vertebra haemal spine. Caudal-fin rays I,6+6,I(1) or I,6+7,I(3), medial rays singly branched; ventral procurrent rays not visible; fin continuous to caudal peduncle, truncate. Parhypural and hypurals 1 and 2 fused, supporting seven or eight rays; hypural 3 fused to hypurals 4 and 5, supporting five rays; neural arch of compound centrum incomplete; uroneural thin, dorsally expanded, supporting two rays. Vertebrae 38 or 39; 1 precaudal, 37 or 38 caudal. One rib.

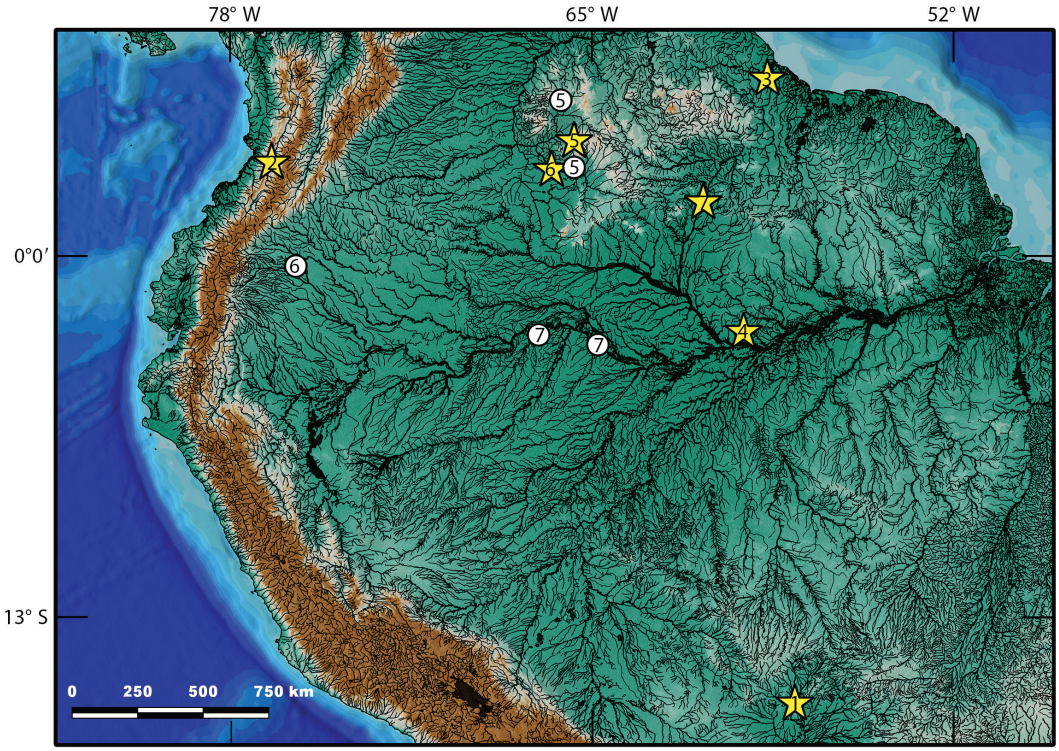

FIGURE 7. Type localities of species of *Paravandellia*: Stars for holotypes; circles, paratypes. 1. *Parav. oxyptera*; 2. *Parav. phaneronema*; 3. *Parav. alleynei*; 4. *Parav. vampyra*; 5. *Parav. oscarleoni*; 6. *Parav.* sp. *brooksi*; 7. *Parav. luna.*

Laterosensory system: Supraorbital sensory canal with paired pores s1, s2, s3, s4, s5, and s6. Infraorbital canal absent. Preopercular sensory canal with single pore. Lateral-line canal short, with three pores, extending from just posterior of opercular patch of odontodes to middle of axillary gland. Superficial neuromasts and papillae not visible.

Coloration in alcohol: Dorsum whitish from nape to caudal-fin base, with paired rows of dark brownish irregular chromatophores lateral to dorsal midline (AUM 57772), or arranged in two parallel rows (AMNH 230907), from just posterior of posterior margin of pectoral fin to just anterior of pelvic-fin origin. Single row of dark brown chromatophores scattered along midline of flank, extending from posterior margin of pectoral fin to just anterior to pelvic-fin base in AMNH 230907. Body chromatophores entirely absent from AUM 56700. Head whitish in dorsal view, with numerous pale brown chromatophores arranged along neurocranium. Eyes black. Small group of dark brown chromatophores surrounding opercular patch of odontodes, at posterolateral corner of head. Ventral surface of head and body whitish, entirely devoid of pigment. Bilateral row of white dorsoventrally elongated lipid masses visible through skin in lateral and ventral views, extending from anterior 25% of body to anal-fin origin (AUM 57772). Fins hyaline.

Distribution (fig. 7): Known only from right-bank (eastern) tributaries of the Upper Orinoco that drain western slopes of the Guiana Shield highlands in Amazonas State, Venezuela.

These include the Guapuche and Yutaje rivers in the Ventuari River basin, and Caño Soromoni, which drains southwestern slopes of Cerro Duida before directly entering the Orinoco River.

Etymology: Species epithet honors Oscar Leon Mata, Ing. RNR, 28 November 1964–25 December 2017, curator of the fish collection of the Museo de Ciencias Naturales in Guanare, Venezuela (MCNG) and dearly missed friend and collaborator of N.K.L. After a childhood spent on Isla Margarita, Oscar became a passionate student of Venezuelan fishes at the Universidad Nacional Experimental de los Llanos Occidentales Ezequiel Zamora (UNELLEZ). There, he developed a thesis on the ornamental fishes of the Upper Orinoco in Amazonas State, where he established strong friendships and a second home in the indigenous community of Macarucu, near the mouth of the Ventuari River. Oscar's leadership of botanical and ichthyological expeditions to Amazonas have left an indelible mark on the scientific understanding of this region's incredible biodiversity, including the collection of specimens supporting this study's descriptions of two new species.

Ecological notes: All specimens collected during day and night at the end of the dry season (March/April) from clearwater to blackwater rivers draining the western Guiana Shield highlands. Substrates varied from cobble and gravel (AUM 57772) to bedrock and sand (AUM 56700).

***Paravandellia brooksi*,** new species

Figures 8, 9, 4E, 5, 6E; table 2

Zoobank registration:urn:lsid:zoobank.org:act:6F8CD6C6-D0CF-4C92-9AF5-9DD868077511

Holotype: AUM 43316, 19.2 mm SL, alc, ct, pm, Venezuela, Amazonas State, Orinoco River right bank at bedrock outcrop 52.9 km SE of San Antonio, 102 km W of La Esmeralda, 3.10036° -66.46277°, ca. 100 m above sea level, N.K. Lujan, D.C. Werneke, M.H. Sabaj, O León Mata, M. Arce, R. Betancur, T.E. Wesley, 04 March 2005, field number VEN05-13.

Paratypes: Two specimens. AUM 54192, 1, 16.8 mm SL, alc, ct, Venezuela, Amazonas State, Ventuari River right bank 157.5 km ESE of Puerto Ayacucho, Caño Maco mouth, right bank tributary of Ventuari River at community of San Francisco de Maco, 4.95591° -66.35066°, ca. 110 m above sea level, J. Birindelli, V. Meza, N.K. Lujan, 14 April 2010, field number VEN10-44. ROM 112354, tissue T29610, 1, 22.9 mm SL, alc, ct, lp, Ecuador, Sucumbios Province, Cuyabeno Canton, Aguarico River upstream of Sabalo Cofán community, -0.3593333° -75.669°, ca. 213 m above sea level, N.K. Lujan, J. Valdaviezo, F. Boily, J. Vicente Montoya, F. Sanchez, G. Echevarria, G. Jijon, 09 April 2022, field number ECU22-15.

Additional nontype material: MZUSP 35612, 1, 26.9 mm SL, alc, ct, Brazil, Rondônia State, Santo Antônio Falls, -8.798511° -63.95118°, ca. 60 m above sea level.

Diagnosis: *Paravandellia brooksi* differs from all congeners by having more medial teeth on premaxilla (fig. 5E; 21 or 22; vs. 10 in *Parav. oscarleoni*, 11 in *Parav. alleynei* and *Parav. vampyra*, 15 in *Parav. phaneronema*, 18–19 in *Parav. oxyptera*, 19–20 in *Parav. luna*); and more principal dorsal-fin rays (11 vs. 8 in *Parav. oxyptera* and *Parav. phaneronema*, 8 or 9 in *Parav. vampyra*, 9

in *Parav. alleynei*, 9–10 in *Parav. oscarleoni* and *Parav. luna*). It further differs from all congeners but *Parav. oxyptera* by having the dorsal-fin first pterygiophore at a vertical anterior to 25th vertebra neural spine (vs. 21st in *Parav. oscarleoni*, 21st, 22nd or 23rd in *Parav. vampyra*, 22nd in *Parav. alleynei* and *Parav. phaneronema*, and 26th–28th in *Parav. luna*); from all congeners except *Parav. phaneronema* by having a shorter posterolateral process of parurohyal, reaching 50% of anterior ceratohyal length (fig. 5E; vs. reaching past 50%); from all congeners except *Parav. luna* by having 25–30 opercular odontodes (fig. 6E; vs. 10–11 in *Parav. vampyra*, 11–15 in *Parav. oscarleoni*, 16–17 in *Parav. alleynei*, 22–26 in *Parav. oxyptera*, and 23–26 in *Parav. phaneronema*). It is further distinguished from *Parav. luna* by having a wider autopalatine fenestra, occupying 75% of its area (fig. 4E; vs. 50%); 18–21 interopercular odontodes (fig. 6E; vs. 16–17) and a straight inner margin of frontal (fig. 4E; vs. serrated); from *Parav. oxyptera* and *Parav. phaneronema* by having a shorter ascending process of opercle, about 70% length of opercular patch of odontodes (fig. 6E; vs. 90% in *Parav. oxyptera* and longer than opercle in *Parav. phaneronema*); and from *Parav. phaneronema* by having 4–5 dentary teeth (fig. 5E; vs. 3).

Description: Morphometric data for holotype and type series presented in table 2.

Gross external morphology: Dorsal profile of body convex from tip of snout to midpoint of dorsum, concave to dorsal insertion of caudal fin. Ventral body profile approximately straight from mouth to anal-fin insertion, convex to insertion of caudal fin. Cross section of body in trunk region approximately oval, becoming gradually more compressed to dorsal-fin base. Caudal peduncle strongly compressed. Axillary gland well developed, with conspicuous pore. Head straight, depressed, approximately triangular in dorsal view. Eye conspicuous, with thin translucent skin covering. Anterior nostril small. Posterior nostril located just anterior to anterior orbital rim, surrounded by fleshy flap on anterior margin. Mouth ventral. Upper lip broad and continuous with lateral margin of head. Nasal barbel absent. Maxillary barbel short, reaching middle of eye. Rictal barbel vestigial. Branchiostegal membrane entirely fused to isthmus.

Skull morphology: Anterior margin of mesethmoid slightly concave, with discrete notch; cornua oriented at 45° to sagittal axis. Cranial fontanel diamond-shaped occupying approximately 75% of skull roof area in dorsal view; delimited anteriorly by mesethmoid and frontal and posteriorly by sphenotic-prootic-pterosphenoid and parietosupraoccipital. Sesamoid supraorbital and antorbital absent. Autopalatine wide, approximately trapezoidal, with conspicuous proximal posteriorly directed process, connected to lateral ethmoid. Autopalatine fenestra wide, occupying about 75% of autopalatine area in dorsal view. Sphenotic, prootic, and pterosphenotic robust and entirely fused to each other. Median premaxilla approximately rectangular, with 20(1) or 21(2) teeth arranged in three rows, anterior row with 8(1) or 9(2), middle row with 8(2) or 10(1), posterior row with 4(3). Parasphenoid small, compact, approximately hexagonal. Anterior portion of Weberian complex fused to basioccipital-exoccipital. Weberian capsule with constricted opening at lateral end of long neck-like collar. Premaxilla anteriorly forked, with 4(1), 5(1), or 8(1) teeth and 2 large distal scalpelloid teeth. Maxilla toothless, wide, approximately 50% as long as premaxilla. Dentary with 4(2) or 5(1) robust, medially curved teeth arranged in two rows, either with each row having 2(2) or outer row with two and inner row with 3(1). Metapterygoid wide, rectangular, with anterior osseous flange. Hyomandibula thin, connected to sphenotic-prootic-

Table 2. Morphometric data for holotype of *Paravandellia brooksi.*

	Holotype
Standard Length	19.2
Body Depth	12.5
Caudal Peduncle Depth	7.8
Body Width	9.9
Caudal Peduncle Width	7.8
Predorsal Length	68.2
Preanal Length	70.8
Prepelvic Length	63.5
Dorsal-fin base length	8.3
Anal-fin base length	9.4
Pectoral-fin length	13.0
Pelvic-fin length	11.5
Head Length	15.6
Head Depth	43.3
Head Width	96.7
Preorbital Length	33.3
Interorbital Width	26.7
Eye Diameter	26.7
Mouth Width	56.7
Interopercular Patch Length	36.7
Opercular Patch Length	30.0

pterosphenoid via cartilage block; lacking conspicuous osseous flange. Articulation between metapterygoid and quadrate through cartilage block. Preopercle long, thin, rectangular, with conspicuous anterior process reaching 20% of quadrate length.

Opercular suspensorium: Opercular patch of odontodes wide, elliptical, located laterally on head; opercular odontodes 25–30, arranged in three irregular rows. Opercle with well-developed dorsally directed ascending process, ca. 70% of opercular patch odontodes length, lacking osseous flange. Interopercular patch of odontodes narrow, with 18 odontodes. Opercular and interopercular odontodes thin, conical, with straight base, gradually compressed distally, tips curved dorsomedially.

Hyoid arch: Four branchiostegal rays, three medialmost rays articulated with anterior ceratohyal, lateralmost ray (ray 4) connected to free connective tissue; ray 4 longest, not aligned with more medial rays, extending laterally between the interopercule and opercule, then posterodorsally along lateral face of opercle (fig. 6E) and medial to the interopercle, ray 3 intermediate in length and curved posterodorsally ventral to opercle, rays 1 and 2 short and straight. Hyoid arch with small ventral

FIGURE 8. Holotype of *Paravandellia brooksi*, AUM 43316, 19.2 mm SL, Venezuela, Amazonas State, Orinoco River right bank at bedrock outcrop 102 km W of La Esmeralda, 3.10036°, -66.46277°, ca. 100 m above sea level, N.K. Lujan, D.C. Werneke, M.H. Sabaj, O. León Mata, M. Arce, R. Betancur, T.E. Wesley, 04 March 2005.

parurohyal having concave anterior margin. Anterolateral horns of parurohyal articulated with posteroventral concavity of ventral hypohyal. Posterolateral processes of parurohyal reaching half of anterior ceratohyal length; posteromedial process reaching first 10% of anterior ceratohyal length. Elongate anterior ceratohyal; short posterior ceratohyal. Dorsal hypohyal and interhyal absent.

Axial skeleton: Pectoral-fin rays I,5; fin approximately triangular, with insertion immediately posterior to opercular membrane; first unbranched pectoral-fin ray not extended as filament. Pelvic-fin rays I,4; fin origin at vertical anterior to 24th vertebra haemal spine; inner fin margins medially separated by interspace. Dorsal-fin rays v,III,8 with eight pterygiophores, first pterygiophore immediately anterior to 25th vertebra neural spine; fin origin posterior to body midpoint. Anal-fin rays iv,II,6 with six pterygiophores; fin origin at vertical through origin of second branched dorsal-fin ray; first anal-fin pterygiophore immediately anterior to 27th vertebra haemal spine. Caudal-fin rays I,6+7,I; ventral procurrent rays 13, dorsal procurrent rays 10; fin continuous to caudal peduncle, forked; medial rays of caudal fin singly branched. Parhypural and hypurals 1 and 2 fused, supporting seven rays; hypural 3 fused to hypurals 4 and 5, supporting five rays; neural arch of compound centrum incomplete; uroneural robust, dorsally expanded, supporting two rays. Vertebrae (excluding Weberian complex) 43; two precaudal, 41 caudal. One rib.

Laterosensory system: Supraorbital sensory canal with paired pores s1, s2, s3, s4, s5, and s6. Infraorbital canal absent. Preopercular sensory canal with single pore. Lateral-line canal short, with three pores, extending from posterior margin of opercle to just above axillary gland pore. Superficial neuromasts and papillae not visible.

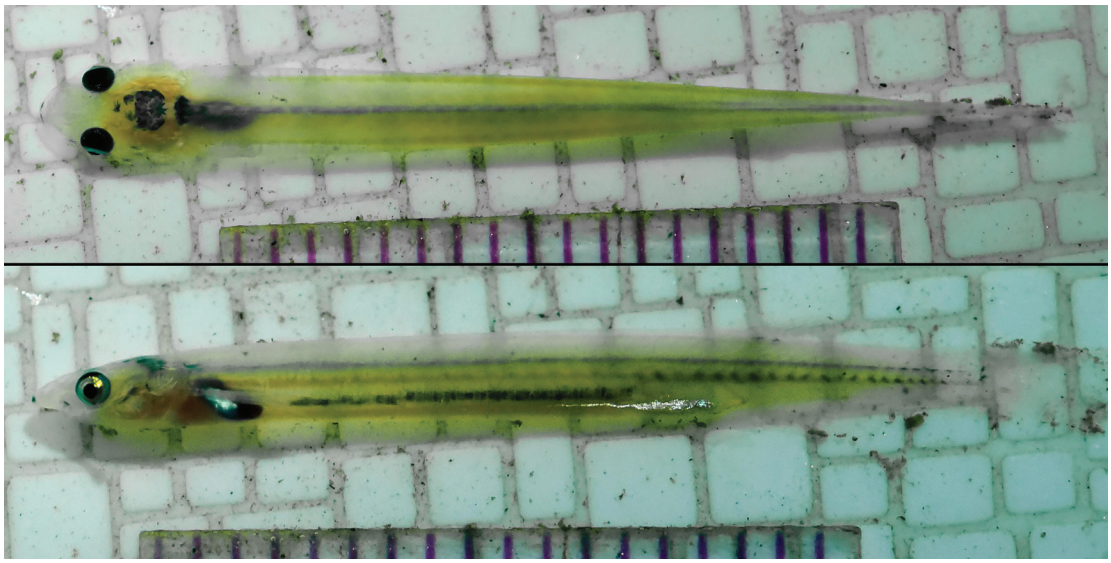

FIGURE 9. Live specimen of *Paravandellia brooksi*, AROM 112354, 22.9 mm SL, Ecuador, Sucumbios Province, Aguarico River upstream of Sabalo Cofán community, -0.3593333°, -75.669°, ca. 213 m above sea level, N.K. Lujan, J. Valdaviezo, F. Boily, J. Vicente Montoya, F. Sanchez, G. Echevarria, G. Jijon, 09 April 2022.

Color in life: Body translucent with vertebrae visible through body wall. Bluish line dorsal to vertebral column corresponding to dorsal nerve tube. Reddish gills and heart. Gut empty, with few flecks of iridescent fat deposits on last quarter of gut. Head clear and yellowish with black eyes. Brain visible through skull foramen and transparent skin as dark purple mass behind eyes. Patches of melanophores on tip of snout and just anterior to eye.

Color in alcohol: Dorsum whitish from nape to caudal-fin base, extending partially down the lateral trunk. In ventral view, pair of yellowish pectoral muscles visible through skin just anterior to anterior gut, visible anteriorly through branchiostegal membrane. Large, dark-brownish patch of gut contents visible midventrally directly posterior to pelvic fins. Head pale whitish in dorsal view. Three well-defined dark chromatophores aligned between tip of snout and anterior margin of eye. Eyes black, partially visible through skin. Dark brown blotches scattered on neurocranium. Ventral view of head whitish. Barbels unpigmented. Fins hyaline.

Distribution (fig. 5): Known from the Upper Orinoco River main channel in southern Venezuela, the Aguarico River main channel in eastern Ecuador near the Peruvian border, and the Madeira River.

Etymology: Species epithet honors American artist David Ian Brooks, born 14 December 1975, for providing critical support to N.K.L. during eight ichthyological expeditions to Ecuador, Guyana, Peru, and Venezuela from 2005 to 2023. Without David's camaraderie and assistance with funding and fieldwork, many thousands of fish specimens, tissues, photos, and associated data could never have been collected. The holotype of *Paravandellia brooksi* was collected just two weeks before N.K.L. and Brooks first met on a bedrock island in the Casiquiare Canal.

Ecological Notes: AUM 43316 was collected from a bedrock shoal in the main channel of the Orinoco River and ROM T29610 was collected during the day by backpack electrofishing shallow sandy substrate in flow in a side channel of the Aguarico River.

***Paravandellia luna*, new species**

Figures 10, 4F, 6F, 7, 11, 12, 13; table 3

Zoobank registration: urn:lsid:zoobank.org:act:41262564-EE4D-41CA-9281-AED47ADB3543

Holotype: UFRJ 14043, 27.6 mm SL, Brazil, Roraima State, beach at Bem-Querer rapids, Branco River drainage, 1.930278 -61.002778, 50 m above sea level, E Henschel, F Rangel-Pereira, P Bragança, 31 August 2019.

Paratypes: ANSP 189307, 1, 23.8 mm SL, alc, ct, Brazil, Amazonas State, Jutai River downstream of Puerto Antunes and upstream of Foz de Jutai, Solimões–Amazon drainage, -2.890556° -66.955°, 42 m above sea level, J.P. Friel, J.G. Lundberg, 13 November 1993. UFRJ 12450, 6, 17.2–29.9 mm SL, all collected with holotype. UFRJ 12451, 24, 16.1–27.9 mm SL, Brazil, Amazonas State, sandbanks in front of Alvarães, Solimões-Amazon drainage, -3.188889 -64.793611, 42 m above sea level, E. Henschel, F. Rangel-Pereira, A. Katz, J. Oliveira, E. Barroso, 14 September 2019.

Diagnosis: *Paravandellia luna* differs from all congeners by having a narrower autopalatine fenestra, occupying about half of autopalatine area (fig. 4F; vs. 75% in *Parav. oxyptera*, *Parav. phaneronema*, and *Parav. brooksi*, and 80% in *Parav. oscarleoni*, *Parav. alleynei* and *Parav. vampyra*); and a wide ascending process of opercle (fig. 6F; vs. thin and elongate). It differs from all congeners except *Parav. oxyptera* and *Parav. brooksi* by having acute processes extending into the posterior cranial fontanel from anterolateral corners of the parietosupraoccipital (fig. 4F; vs. adnate to sphenotic in *Parav. alleynei*, absent in *Parav. phaneronema* and *Parav. oscarleoni*).

Description: Morphometric data for holotype and type series presented in table 3.

General Morphology: Dorsal profile of body convex from tip of snout to dorsal-fin insertion, straight to dorsal insertion of caudal fin. Ventral body profile approximately straight from mouth to anal-fin insertion, concave to caudal-fin insertion. Cross section of body in trunk region approximately oval, becoming gradually more compressed to dorsal-fin base. Caudal peduncle strongly compressed. Axillary gland well developed, with conspicuous pore.

Head straight, depressed, approximately triangular in dorsal view. Eye conspicuous, with thin translucent skin covering. Anterior nostril small; posterior nostril aligned to anterior orbital rim, surrounded by fleshy flap on anterior margin. Mouth ventral. Upper lip broad, continuous with lateral margin of head. Nasal barbel absent; maxillary barbel short, reaching posterior margin of eye; rictal barbel vestigial. Branchiostegal membrane entirely fused to isthmus.

Skull anatomy: Anterior margin of mesethmoid straight, with discrete notch; cornua oriented at 65° angle to sagittal axis. Cranial fontanel diamond shaped, occupying approxi-

Table 3. Morphometric data for holotype and paratypes (n = 10) of *Paravandellia luna*.

	Holotype	Min	Max	Mean
Standard Length	25.3	25.1	27.4	26.2
Body Depth	9.5	7.7	12.0	9.8
Caudal Peduncle Depth	5.5	4.0	5.7	5.2
Body Width	7.5	6.5	9.4	8.0
Caudal Peduncle Width	1.6	1.1	2.6	1.7
Predorsal Length	73.9	72.2	77.1	73.8
Preanal Length	76.3	73.4	78.1	75.9
Prepelvic Length	65.2	63.5	72.1	68.6
Dorsal-fin base length	5.9	5.3	8.2	6.2
Anal-fin base length	5.9	5.0	6.7	5.8
Pectoral-fin length	7.9	7.7	11.2	8.6
Pelvic-fin length	4.7	4.7	6.1	5.5
Head Length	11.9	10.9	12.0	11.4
Head Depth	53.3	37.9	56.7	47.6
Head Width	80.0	76.7	93.3	85.7
Preorbital Length	36.7	34.5	43.3	39.0
Interorbital Width	26.7	23.3	36.7	30.0
Eye Diameter	23.3	23.3	33.3	28.0
Mouth Width	26.7	26.7	36.7	31.7
Interopercular Patch Length	30.0	20.0	31.3	27.7
Opercular Patch Length	30.0	26.7	33.3	28.6

mately 75% of skull roof area; delimited anteriorly by mesethmoid and frontal and posteriorly by sphenotic-prootic-pterosphenoid and parietosupraoccipital. Frontals with serrated medial expansions. Sesamoid supraorbital and antorbital absent. Autopalatine wide, approximately rectangular, with conspicuous proximal process posteriorly directed, connected to lateral ethmoid. Autopalatine fenestra wide, occupying approximately half its area. Sphenotic, prootic, and pterosphenotic robust, entirely fused to each other. Median premaxilla approximately trapezoidal, with 20 teeth arranged in three rows; anterior row with eight, middle row with eight, posterior row with four. Parasphenoid small, compact, approximately hexagonal. Anterior portion of Weberian complex fused to basioccipital-exoccipital. Weberian capsule with constricted opening at distal end of long, necklike collar. Premaxilla anteriorly forked, with three to six medial teeth and two or three large, distal scalpelloid teeth. Maxilla toothless, wide, approximately half as long as premaxilla. Dentary with four robust, medially curved teeth arranged in a single distal patch. Metapterygoid wide, rectangular, lacking anterior osseous flange. Hyomandibula thin, connected to sphenotic-prootic-pterosphenoid via cartilage block, lacking

FIGURE 10. Holotype of *Paravandellia luna*, UFRJ 14043, 27.6 mm SL, Brazil, Roraima State, beach at Bem-Querer rapids, Branco River drainage, 1.930278°, -61.002778°, 50 m above sea level, E. Henschel, F. Rangel-Pereira, P. Bragança, 31 August 2019. Photo by Axel Katz.

conspicuous osseous flange. Articulation between metapterygoid and quadrate through cartilage block. Preopercle long, thin, rectangular, with conspicuous anterior process reaching 10% of quadrate length.

Opercular suspensorium: Opercular patch of odontodes wide, elliptical, located laterally on head, with 26 to 30 odontodes arranged in four irregular rows. Opercle with well-developed dorsally directed ascending process ca. 70% length of opercular patch of odontodes, lacking osseous flange. Interopercular patch of odontodes narrow, with 15–17 odontodes. Opercular and interopercular odontodes thin, conical, with straight base, gradually compressed distally, with tips curved dorsomedially.

Hyoid arch: Four branchiostegal rays, two medialmost rays (1 and 2) articulated with anterior ceratohyal, rays 3 and 4 articulated with posterior ceratohyal; ray 4 longest, not aligned with more medial rays, extending laterally between the interopercule and opercule, extending posterodorsally along lateral face of opercle (fig. 6F) and medial to the interopercle, rays 1–3 curved laterodorsally ventral to opercle. Hyoid arch with small ventral parurohyal having concave anterior margin. Anterolateral horns of parurohyal articulated with posteroventral concavity of ventral hypohyal. Posterolateral processes of parurohyal reaching half of anterior ceratohyal length; posteromedial process reaching first quarter of anterior ceratohyal length. Elongate anterior ceratohyal, short posterior ceratohyal. Dorsal hypohyal and interhyal absent.

Axial skeleton: Pectoral-fin rays I,5 or I,6; fin approximately triangular, with insertion immediately posterior to opercular membrane; first unbranched ray not extended as filament.

FIGURE 11. Paratype of *Paravandellia luna*, UFRJ 12451, 27.7 mm SL, Brazil, Amazonas State, sandbanks in front of Alvarães, Solimões-Amazon drainage, -3.188889°, -64.793611°, 42 m above sea level, E. Henschel, F. Rangel-Pereira, A. Katz, J. Oliveira, E. Barroso, 14 September 2019. Photo by Axel Katz.

Pelvic-fin rays I,4; fin origin at vertical anterior to 24th or 25th vertebra haemal spine; inner fin margins medially separated by interspace. Dorsal-fin rays iv-v,II,7-8 with eight pterygiophores, first pterygiophore immediately anterior to 26th or 28th vertebra neural spine; fin origin posterior to midbody. Anal-fin rays iii-iv,II,5 with six pterygiophores; tip of first anal-fin pterygiophore immediately anterior to 25th–28th vertebra haemal spine; fin origin at vertical through origin of first or second branched dorsal-fin ray. Caudal-fin rays I,6+7,I, medial rays singly branched; ventral and dorsal procurrent rays 12–15; fin continuous to caudal peduncle, slightly forked. Parhypural and hypurals 1 and 2 fused, supporting seven rays; hypural 3 supporting two rays; hypurals 4 and 5 supporting two rays; neural arch of compound centrum incomplete; uroneural robust, dorsally expanded, supporting two rays; hypurapophysis present. Vertebrae (excluding Weberian complex) 45 or 46; two precaudal, 43 or 44 caudal. One rib.

Laterosensory system: Supraorbital sensory canal having paired pores s1, s2, s3, s4, s5, and s6. Infraorbital canal absent. Preopercular sensory canal having single pore. Lateral-line canal short, with three pores, extending from posterior margin of opercle to 75% of pectoral-fin length. Superficial neuromasts and papillae not visible.

Color in Life: Body whitish with vertebrae visible through body wall. Reddish gills and heart. Gut distended with blood, with few flecks of iridescent fat deposits on last quarter of gut. Head clear and whitish with black eyes. No melanophores visible on body.

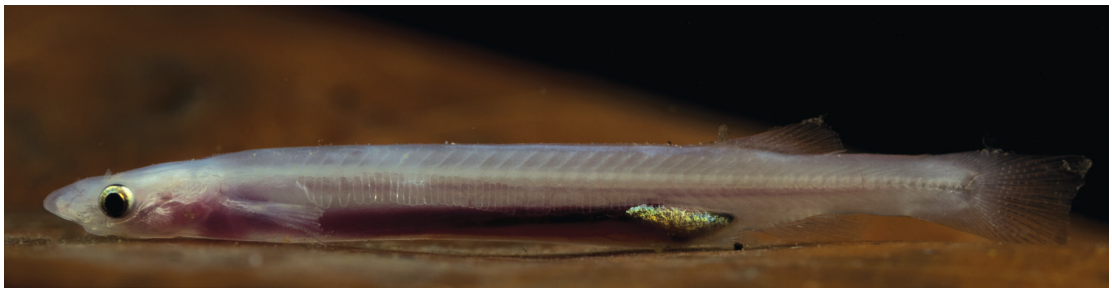

FIGURE 12. Live specimen of *Paravandellia luna*, UFRJ 12450, ca. 20 mm SL, Brazil, Roraima State, beach at Bem-Querer rapids, Branco River drainage, 1.930278°, -61.002778°, 50 m above sea level, E. Henschel, F. Rangel-Pereira, P, Bragança, 31 August 2019.

Color in Alcohol: Dorsum whitish from nape to base of tail, extending partially down the lateral trunk. In ventral view, pair of yellowish pectoral muscles visible through skin just anterior to anterior part of gut. Yellowish patch of gut contents visible midventrally, directly posterior to pelvic fins in some specimens. Head pale whitish in dorsal view. Eyes black, visible through skin. Well-defined dark brown blotches scattered on surface of neurocranium. Ventral view of head whitish. Barbels unpigmented. Fins hyaline.

Distribution: Known from the Branco and Solimões river drainages, Amazon River basin.

Etymology: Name references both the white color of living individuals and an indigenous Amazonian tale in which the Moon, forbidden to marry the Sun, copiously cried. The Moon's tears ran from the land to the sea, which rejected such a massive amount of water. Thus, these tears carved several river channels into northern South America, including that of the Amazon (Rodrigues, 1890).

Ecological Notes (fig. 11): Specimens were collected exclusively at night in the sand of sandbanks near the river margin, at about 1 m water depth along with individuals of *Haemomaster venezuelae* Myers, 1927, suggesting a nocturnal habit. Similar collecting efforts during the day did not succeed in capturing specimens, suggesting that they might be deeper buried in sand or in deeper sandbanks avoiding sunlight.

DISCUSSION

Generic Assignments and the Differential Diagnoses of *Paravandellia* and *Paracanthopoma*

The most comprehensive examination of generic limits between *Paravandellia* and *Paracanthopoma* was the recent review of *Paracanthopoma* by de Pinna and Dagosta (2022), in which nine morphological synapomorphies were proposed for each genus. However, these features require further explanation, with some ambiguously defined or exhibiting overlapping conditions across species currently assigned to *Paravandellia* and *Paracanthopoma*. Ideally, diagnostic character states should follow a logical order (e.g., Sereno, 2007) in which synapomorphies are distinguished from symplesiomorphies through formal phylogenetic optimization. As we lack such analysis, we seek to recognize and reinforce as many diagnostic character states as possible by placing the states proposed by

FIGURE 13. Type locality and collection of *Paravandellia luna* Bem-Querer Rapids, Branco River, Amazon River basin, Caracaraí, Roraima, Brazil.

de Pinna and Dagosta (2022) in the context of historical changes in conceptual boundaries for each taxon and patterns of character variation across species, regardless of evolutionary history.

First, the branchiostegal velum, exclusive to *Paracanthopoma*, consists of a free integumentary fold across the isthmus that lacks branchiostegal rays, likely a derivative of the branchiostegal membrane (de Pinna and Dagosta, 2022). Our observations of ethanol-preserved specimens confirm this condition, i.e., that this structure is distinct from the free branchiostegal membrane seen in other trichomycterids as it lacks branchiostegal rays associated with it. Developmental data to inform the origin and topology of the branchiostegal velum as a neomorph and definitive evidence of monophyly. and its relationship to the branchiostegal membrane are lacking; however, a paralectotype of *Parac. parva* (BE-RBINS VER-FIS 602) exhibits a branchiostegal velum medially fused to the isthmus (Henschel et al., 2021b; fig.3C), a condition treated by de Pinna and Dagosta (2022) as an exception (i.e., a deformity) without further justification. They support this idea by stating that this condition of the velum is "a low frequent-variant occasionally seen in available samples" (de Pinna and Dagosta, 2022: 76), but give no information about which species, lots, specimens, or localities these are. Hence, their definition of the velum and its potential value as a diagnostic character remains unclear. The significance of this putative deformity remains to be investigated and considered before regarding the "branchiostegal velum" as evidence of monophyly of *Paracanthopoma.*

For de Pinna and Dagosta (2022), the second conspicuous condition distinguishing *Paracanthopoma* from *Paravandellia* is presence in the former of well-developed bilateral flanges on the dorsal border of the posteromedial notch (or recess) on the median premaxilla. As those authors noted, these dorsal bilateral flanges are also seen in *Parav. phaneronema* but to a lesser degree—a condition they considered an "incipient homologous state," also without definition or elaboration. We confirm presence of these bilateral flanges not only in *Parav. phaneronema*, but also in *Parav. brooksi* (fig. 4E). On the other hand, *Parac. malevola* lacks well-developed paired flanges on the dorsal surface of the median premaxilla (de Pinna and Dagosta, 2022: fig. 26B), displaying a condition similar to that seen in other species of *Paravandellia*. Similarly, de Pinna and Dagosta (2022) stated that a well-defined posteromedial recess on the median premaxilla is the third diagnostic character of *Paracanthopoma*; however, species of *Paravandellia* also exhibit such a recess, though in the miniature species *Parac. saci* and *Parac. malevola* the recess is less conspicuous than in putative congeners (de Pinna and Dagosta, 2022: figs. 26B, 34C). Thus, bilateral dorsal flanges and a posteromedial recess on the median premaxilla are variably present in both genera, reducing these characters' diagnostic value and suggesting rather that they support their close intrageneric relationship.

A distally forked maxilla is the fourth condition regarded by de Pinna and Dagosta (2022) as diagnostic for *Paracanthopoma.* However, the authors neither illustrated nor described the maxilla of *Parac. ahriman*, *Parac. irritans*, *Parac. malevola*, and *Parac. satanica.* Our analysis of CT-imagery of *Parac. malevola* (MCP 36221, MCP 36223) confirms the presence of a forked maxilla, whereas *Parac. irritans* (MCP 36219) has a blunt unforked distal margin of the premaxilla. Comparative material of *Parac. ahriman* and *Parac. satanica* was unavailable to us. Thus, the distribution and value of this condition awaits further confirmation. A posterior articular process of the autopalatine oriented parallel to the neurocranium is the fifth character said to be diagnostic, yet is variable within *Paracanthopoma*. For example, in *Parac. saci*, the posterior process is oriented obliquely slightly away from the neurocranium, while in *Parac. malevola* it is oriented obliquely slightly toward the neurocranium (de Pinna and Dagosta 2022: figs. 26A, 34B).

De Pinna and Dagosta (2022) considered a deeply indented anterior margin of the autopalatine as the sixth diagnostic condition of *Paracanthopoma*, as first noted by DoNascimiento (2012). However, as the authors themselves noted, this autopalatine morphology was seen on the right side of a specimen of *Parav. phaneronema* they examined (de Pinna and Dagosta, 2022: fig. 46B) and was considered an abnormality without further justification. De Pinna and Dagosta (2022) further distinguish *Paracanthopoma* from *Paravandellia* based on composition of the mandibular coronoid process, their seventh diagnostic character of *Paracanthopoma*. They state that in the former it is formed mainly by the dentary, but in the latter it is formed by the retroanguloarticular alone, yet in CT-imagery herein of *Parav. oxyptera* and *Parav. luna* the coronoid process clearly has a more robust dentary component (fig. 5B, F).

The eighth putatively diagnostic character state proposed by de Pinna and Dagosta (2022) for *Paracanthopoma* is absence of the upper pharyngeal tooth plate. However, this condition was dismissed in the previous work by DoNascimiento (2012), where he examined two new but unde-

scribed *Paravandellia* species from the Caquetá and Orinoco river basins that also lack the upper pharyngeal tooth plate (DoNascimiento, 2012: 169). The last character listed by de Pinna and Dagosta (2022) to distinguish *Paracanthopoma* is the restricted joint between the neural arch of the complex vertebra and parietosupraoccipital (first proposed by DoNascimiento, 2012: 90). Although confirmed by us in all species that we currently consider valid members of *Paracanthopoma*, an undescribed species that exhibits most of this genus's diagnostic character states as proposed by de Pinna and Dagosta (2022) lacks this condition (ROM 87072). Instead, the joint between the anterior margin of the complex vertebra and the posterior margin of the parietosupraoccipital consists of a fine line of cartilage along the entire boundary between these bones.

In addition to a small median notch on the mesethmoid bordered by small dorsal flanges and the coronoid process formed exclusively by the retroanguloarticular in *Paravandellia*, de Pinna and Dagosta (2022) proposed another six diagnostic character states for this genus. First, their proposal of a narrow ventral strut of the orbitosphenoid is based on a character originally proposed by DoNascimiento (2012: 69), who stated that the "size of the optic foramen" could be wide (as seen in *Paravandellia* and *Vandellia*) or reduced (all other trichomycterids). In contrast to de Pinna and Dagosta (2022), who do not quantify the diagnostic limits of strut narrowness, DoNascimiento (2012) defined a wide optic foramen as having a diameter greater than 25% of the orbitosphenoid's lateral surface, thus resulting in a narrow ventral strut. Second, still focusing on orbitosphenoid anatomy, de Pinna and Dagosta (2022) propose that a wide space between the posterior margin of this bone and the anterior margin of the sphenotic-prootic-pterosphenoid is diagnostic for *Paravandellia.* Again, the term "wide" is subjective and the character is based on one originally proposed by DoNascimiento (2012: 71), who refers to it as the "articulation between the posteroventral margin of the orbitosphenoid and prootic." However, *Parac. cangussu* also exhibits a markedly separated orbitosphenoid and prootic (de Pinna and Dagosta 2022: fig. 12A, C), and thus not beingdiagnostic of *Paravandellia*. Third, another supposedly diagnostic condition of *Paravandellia* proposed by de Pinna and Dagosta (2022) is absence of an anterior flange on the dorsal process of the opercle, although *Parac. truculenta* exhibits this same opercular anatomy (de Pinna and Dagosta, 2022: fig. 41A). Fourth, our analysis of CT-imagery and illustrations of *Paravandellia* species in de Pinna and Dagosta (2022) reveals that the presence of a bony expansion of the opercle, covering its articulation with the hyomandibula, is not exclusive of this genus, being also found in *Parac. malevola* and *Parac. irritans* (de Pinna and Dagosta, 2022: figs. 23A, 26A). Fifth, these authors state that widely separated anterior processes of the parurohyal, with an interspace at least 3× their length, is exclusive of *Paravandellia*; however, measurements from their illustrations show these processes to be separated by a distance of 5.25× their length in *Parac. vampyra*, and a distance of 3.6× their length in *Parac. ahirman* (de Pinna and Dagosta, 2022: figs. 7C, 43C). Finally, an absent or cartilaginous fourth ceratobranchial is the last of nine features proposed by de Pinna and Dagosta (2022) as diagnostic of *Paravandellia.* However, they report a personal communication from DoNascimiento noting that five specimens of *Paracanthopoma* from the Orinoco River basin lack the fourth ceratobranchial, a condition that de Pinna and Dagosta (2022) speculate is homoplastic, though without a formal phylogenetic analysis.

It seems that many diagnostic characteristics of *Paracanthopoma* and *Paravandellia* overlap, reinforcing the need to reappraise diagnostic characters in light of phylogeny and ontogeny. The branchiostegal velum demands ontogenetic assessment to confirm it as either a neomorph or homolog with the branchiostegal membrane. Despite the extensive and laudable effort by de Pinna and Dagosta (2022) to clearly define limits for *Paracanthopoma* and *Paravandellia*, one clearly visible and historically important character state was given insufficient consideration: absence or presence of an isolated medial patch of teeth on the premaxilla. Upper jaw dentition of most vandelliines is restricted to a patch of teeth on the median premaxilla and the distal patch of scalpelloid teeth on the premaxilla, the latter being synapomorphic for the subfamily. However, many species, spanning both *Paracanthopoma* or *Paravandellia*, exhibit an additional patch of slender, hook-shaped teeth on the medial end of the premaxilla, immediately lateral to the median premaxilla (fig. 5; Henschel et al., 2021: fig. 8B).

Median premaxillary teeth have been treated in the past by several authors. Miranda-Ribeiro, when describing *Parav. oxyptera*, mentioned that it has "dentes n'uma serie nos maxillares e n'um facho nos intermaxillares" (Miranda-Ribeiro, 1917: 29), referring to the series of medial teeth on the premaxilla and the patch of teeth on the median premaxilla. Moreover, in the original descriptions of *Branchioica bertoni*, *Pleurophysus hydrostaticus* Miranda-Ribeiro, 1918, and *Parabranchioica teaguei* (all junior synonyms of *Parav. oxyptera*; de Pinna and Wosiacki, 2003), presence of a medial patch of teeth on the premaxilla is specifically mentioned. This condition was also considered by Eigenmann (1918) as exclusive to *Paravandellia* and *Branchioica*. Schmidt (1993), in the first cladistic analysis examining relationships among vandelliines, also considered the presence of medial teeth on the premaxilla as exclusive to *Paravandellia.* On the other hand, the original description of *Parac. parva* by Giltay (1935) and examination of its type series and redescription by Henschel et al. (2021b) confirmed that *Paracanthopoma* lacks these teeth. Our examination of additional CT-imagery of *Parav. oxyptera* and one specimen (BMNH 1944.3.3.10) collected by G.W. Teague from the Uruguay River near Paysandú, and labeled as a cotype of *Parabranchioica teaguei*, confirmed presence of these teeth (fig. 5B). Eight specimens comprised the type series of *Parabranchioica teaguei*, assumed to be deposited at MHNM Montevideo, but were reported as "unknown" by de Pinna and Wosiacki (2003). Unfortunately, the type series of *Parav. oxyptera* was not available to us. Given the repeated and generally consistent historical treatment of medial premaxillary teeth as diagnostic of *Paravandellia* (Baskin, 1973; Schmidt, 1993; DoNascimiento, 2012), we emphasize the importance of considering this exclusive character state as a means for differentiating *Paravandellia* from *Paracanthopoma*. Indeed, we use this character state as the basis for the following discussion of the taxonomic boundaries of *Paravandellia.*

Paravandelia alleynei and *Paravandellia vampyra*

As this study and that of DoNascimiento (2012) consider the presence of a medial patch of teeth on the premaxilla as diagnostic of *Paravandellia*, the composition of *Paracanthopoma* and *Paravandellia* requires revision. Schmidt (1993) examined a poorly cleared and stained

specimen of a vandelliine (AMNH 72899SW), in which the presence of medial teeth on the premaxilla went unnoticed. Moreover, an ethanol-preserved specimen of the same lot (AMNH 72898) has an enlarged axillary gland and a free branchiostegal membrane across the isthmus. These characters led Schmidt (1993) to identify these vandelliines as *Parac. parva*. However, subsequent examination of CT-imagery of AMNH 72898 by Henschel et al. (2021b) confirmed presence of a few small, thin teeth in a patch at the medial end of the premaxilla. This specimen also has a laterally expanded pterosphenoid, extending beyond the sphenotic, a character proposed by DoNascimiento (2012), as exclusive for *Paravandellia*. These characters were used to support the description of *Parav. alleynei*, its placement in *Paravandellia*, and an assertion that the branchiostegal membrane free across the isthmus should not be regarded as diagnostic of *Paracanthopoma*, being found in species of both *Paracanthopoma* and *Paravandellia* (Henschel et al., 2021b).

A year after its description, de Pinna and Dagosta (2022) moved *alleynei* to *Paracanthopoma* based on their revised interpretations and diagnoses of *Paravandellia* and *Paracanthopoma*. Moreover, they described *Parac. vampyra*, a species morphologically similar to *Parac. alleynei* based partly on the presence of medial premaxillary teeth and multiple scalpelloid teeth stacked in parallel, laterally decreasing in size (de Pinna and Dagosta, 2022). The latter condition is also found here in *Parav. oscarleoni*. They asserted that *Parac. alleynei*, *Parac. vampyra*, and species of *Paravandellia* "retained" medial conical teeth on the premaxilla, which also contradicts some of their other observations about vandelliine dentition. One of these other observations is their proposal of the term "scalpelloid teeth" to refer to the "claw-like" premaxillary teeth of vandelliines, a structure that has been historically regarded as a key morphological innovation of hematophagous candirus, being highly modified from the premaxillary dentition seen in other trichomycterids and siluriforms (Baskin, 1973; Schmidt, 1993; de Pinna, 1998; DoNascimiento, 2012). However, when discussing the distribution of scalpelloid teeth among vandelliines, de Pinna and Dagosta (2022: 81) state that *Paracanthopoma* + *Paravandellia* exhibit an apomorphic condition when compared to *Vandellia* + *Plectrochilus*, i.e., the scalpelloid teeth of the first two are restricted to the distal margin of the premaxilla, while in the second two, scalpelloid teeth are found along a wider area of the bone, similar to the condition of premaxillary teeth distribution in other trichomycterids and catfishes. Stating that scalpelloid tooth distribution in *Plectrochilus* + *Vandellia* is similar to that in other catfishes implies that scalpelloid teeth are homologous to the premaxillary dentition of other catfishes, as stated in previous studies. However, they also consider the medial teeth on the premaxilla of *Paravandellia* species to be homologous to the premaxillary dentition of other catfishes (de Pinna and Dagosta, 2022: 83), thus creating a confusing scenario where *Paravandellia* has two sets of distinct premaxillary teeth (i.e., the scalpelloid teeth and the medial patch) that share the same origin and are located on the same bone. We agree with previous studies that consider the distal, scalpelloid premaxillary teeth of vandelliines to be modified structures (e.g., Baskin, 1973; DoNascimiento, 2012) and consider the homologies of the medial premaxillary teeth of *Paravandellia* unclear, but still useful to diagnose this genus as proposed by Schmidt (1993).

Moreover, our observations of CT-imagery of *Parav. oxyptera*, *Parav. brooksi*, and *Parav. luna* reveal two large scalpelloid teeth stacked in parallel and two smaller teeth inserted just behind. *Paravandellia phaneronema* is the only species of the genus that has only two large scalpelloid teeth (fig. 4E). Thus, it appears that having more than two fully formed scalpelloid teeth can be informative for diagnosing some species of *Paravandellia*. Given these observations, we return *Paravandellia alleynei* Henschel et al., 2021, to *Paravandellia* and consider *Paracanthopoma vampyra* de Pinna and Dagosta, 2022, to be a congener, yielding *Paravandellia vampyra* (de Pinna and Dagosta 2022), new combination.

Finally, there is a novel, informative character state that previous works on vandelliine systematics have ignored. This is the lateralmost branchiostegal ray (ray 4) elongated, not aligned with the other rays, extending laterally from between the interopercle and opercle, and dorsally lateral to the lateral face of the opercle to beyond and at least partially lateral to the opercular odontodes themselves in all species of *Paravandellia* (fig. 6). This character state can be seen in de Pinna and Dagosta's (2022) illustrations of *Parav. alleynei*, *vampyra*, and *phaneronema* (their figs. 10, 43B, C, and 46, respectively), but is absent in all their other illustrated specimens. Although this branchiostegal ray is elongated in other trichomycterids, this extreme degree of elongation and unique position lateral to the opercle and opercular odontodes is exclusively observed in *Paravandellia* as here defined. Thus, we include this characteristic in our revised diagnosis of the genus, defined as the presence of medial teeth on the premaxilla and the lateralmost branchiostegal ray extending laterodorsally lateral to the opercular odontodes. It is plausible that this branchiostegal condition plays a novel role in opercular function, though further investigation of its possible function is needed. When the opercular odontodes of a cleared and stained specimen are manually erected using a dissecting needle, the distal end of the 4th lateralmost ray slides forward away from its position over the odontodes (J.N.B., personal obs.). Upon opercular eversion, the distal end of the ray is displaced anteriorly from over the odontodes, potentially functioning to clear the odontodes and thus aid in host attachment or detachment. The condition of this branchiostegal ray extending laterally from between the interopercular and opercular bones appears to be unique among Siluriformes, if not Actinopterygii as a whole.

Relationships among Species of *Paravandellia*

Here, we conclude that *Paravandellia* currently contains seven species: *Parav. oxyptera*, *phaneronema*, *alleynei*, *vampyra*, new combination, *oscarleoni*, *brooksi*, and *luna*.

Within *Paravandellia*, many character states that might previously have supported allocation of a species to *Paracanthopoma* suggest that *Parav. oscarleoni*, *Parav. alleynei*, and *Parav. vampyra* are more closely related to each other than to congeners. These character states include their free fold of skin across the isthmus, lack of a notch on the anterior margin of the mesethmoid, posteriorly directed opercular odontodes, and an anterior osseous flange on the ascending process of opercle (fig. 4A, 5A, 6A). In their description of *Parav. vampyra* as a new species of *Paracanthopoma* and their discussion of *Paracanthopoma* interrelationships, de Pinna and Dagosta (2022)

hypothesize that *Parav. vampyra* and *Parav. alleynei* are more closely related to each other than to congeners based on their distinctive, shared orientation of the mesethmoid cornua at a 45° angle or less to the sagittal axis, and their multiple aligned scalpelloid teeth. Within *Paravandellia*, these characters remain useful in diagnosing a putative clade composed of these two species plus *Parav. oscarleoni*. These three species also exhibit fewer teeth on the median premaxilla (11 or fewer) and a well-developed osseous flange on the anteromedial margin of the hyomandibula (a homoplastic condition seen in other trichomycterids). Within this group, *Parav. oscarleoni* and *Parav. vampyra* exclusively share five character states: (1) absence of an anteromedial process of the autopalatine; (2) presence of a longer anterior margin of the mesethmoid; (3) median premaxilla wider than long; (4) parasphenoid approximately 3× longer than wide; (5) well-developed anterior margin of the parietosupraoccipital (fig. 4D, 5D, 6D).

The remaining *Paravandellia* species (*oxyptera*, *phaneronema*, *brooksi*, and *luna*) also exclusively share five character states: (1) dorsally oriented opercular odontodes, (2) a notch on the anterior margin of the mesethmoid, (3) a greater number of teeth on the median premaxilla (>15), (4) median premaxilla wider than long, and (5) posterior margin of the premaxilla blunt or slightly forked.

Comments on the Geographical Distributions of *Paravandellia* Species

The recent history of species descriptions and redefinitions of the generic limits of *Paravandellia* provide a complex scenario for inferring the geographic distribution of its species. Most specimens collected in the Paraguay, Uruguay, and Paraná river systems are clearly identifiable as *Parav. oxyptera*, populations found throughout the Amazon, Orinoco, Essequibo, and other river basins are regarded as *Parav.* spp., lacking a clear taxonomic assignment. This is because *Parav. oxyptera* is considered a widespread species in rivers immediately south of the Amazon drainage (i.e., the La Plata River basin). Here, we examined specimens of *Parav. oxyptera* from the Uruguay and Paraná river basins, in addition to a possible type specimen of *Parabranchioica teaguei* and specimens of *Branchioca bertoni* (from the Paraguay River basin), both junior synonyms of *Parav. oxyptera*, to confirm the broad geographic distribution of this species within the La Plata basin. The second long-recognized congener *Parav. phaneronema* has been regarded as restricted to the Upper Cauca basin (de Pinna and Wosiacki, 2003), though it was collected in the Baudo River along Colombia's Pacific Coast for the first time in 2019 by N.K.L. and Armando Ortega-Lara. Our μCT-comparison of an individual from this Pacific population with a topotype from the Cauca confirms their indifferentiable skeletal anatomy.

The other five species of *Paravandellia* are distributed throughout rivers in the Guiana Shield (fig. 7). *Paravandellia alleynei* is found in the Essequibo and Branco river basins (Henschel et al., 2021b), and the type series of *Parav. vampyra* was collected from along the Negro River basin (de Pinna and Dagosta, 2022). *Paravandellia oscarleoni* is restricted to the Ventuari-Orinoco River system. *Paravandellia luna* occurs in whitewaters of the Branco River basin and the Japurá drainage, a tributary of the Amazon River at the southernmost limit of the Guiana Shield. *Paravandellia brooksi* exhibits the most disjunct distribution of the genus: its holotype is from the upper Orinoco River

main channel, whereas a paratype is from the Aguarico River, a tributary of the Napo River in eastern Ecuador, and an additional specimen was collected in the Madeira River basin. Additional specimens and genetic analyses are needed to test these morphology-based inferences.

To summarize, we consider *Paravandellia* distinct from all other genera of Vandelliinae by the presence of medial teeth on the premaxilla and the lateralmost branchiostegal ray not aligned with the other rays, extending dorsolaterally lateral to the opercle and opercular odontodes. *Paravandellia* consists of two diagnosable groups that require confirmation by formal phylogenetic analyses: the first composed by *Parav. oscarleoni*, *Parav. alleynei*, and *Parav. vampyra* and the second by *Parav. oxyptera*, *Parav. phaneronema*, *Parav. brooksi* and *Parav. luna*. Further taxonomic and phylogenetic studies directed at *Paravandellia* will undoubtedly reveal additional diversity, and improve our understanding of relationships, diagnoses and biogeographic patterns.

ACKNOWLEDGMENTS

The authors thank Scott Schaefer, Rad Arrindell, Tom Vigliotta, and Chloe Lewis (AMNH), Jonathan Armbruster and David Werneke (AUM), Oliver Crimmen and James Maclaine (BMNH), Roberto Reis (MCP), Mary Burridge, Marg Zur, and Don Stacey (ROM), and Wilson Costa (UFRJ) for facilitating access to specimens deposited in their institutions. Axel Katz (UFRJ) kindly photographed fixed specimens of *Parav. luna*. This work was supported by Conselho Nacional de Desenvolvimento Científico e Tecnologico (CNPq: grant 152240/2022-5 to EH), National Geographic Society (Early Career Grant Number EC-316R-18 to E.H.). N.K.L. is supported by an NSERC Discovery Grant and conducted fieldwork with support from the Coypu Foundation, National Geographic, the Belgian Development Cooperation (DGD) via WWF-Ecuador, and the Universidad de las Americas. Collection of the CT-imagery was supported by a Gerstner Bioinformatics Postdoctoral Fellowship to N.K.L. at AMNH, and was facilitated by CT technicians Morgan Chase at AMNH and Alexander Tinius at the University of Toronto. We thank the following University of Toronto undergraduate students for assisting with CT-segmentation: Eunice Huang, Alice Lo, Jolie Nguyen, Amina Sharif, Christine Tang, Chunnan Yue.

REFERENCES

Abràmoff, M.D., P.J. Magalhães, and S.J. Ram. 2004. Image processing with ImageJ. Biophotonics International 11 (7): 36–42.

Alexander, R.M. 1966. Structure and function in the catfish. Journal of Zoology 148 (1): 88–152.

Baskin, J.N. 1973. Structure and relationships of the Trichomycteridae. Ph.D. dissertation, Department of Ichthyology, City University of New York.

Baskin, J.N., T.M. Zaret, and F. Mago-Leccia. 1980. Feeding of reportedly parasitic catfishes (Trichomycteridae and Cetopsidae) in the Rio Portuguesa Basin, Venezuela. Biotropica: 182–186.

Bockmann, F.A., and I. Sazima. 2004. *Trichomycterus maracaya*, a new catfish from the upper rio Paraná, southeastern Brazil (Siluriformes: Trichomycteridae), with notes on the *T. brasiliensis* species-complex. Neotropical Ichthyology 2 (2): 61–74.

Bonato, K.O., P.C. Silva, and L.R. Malabarba. 2018. Unrevealing parasitic trophic interactions—a molecular approach for fluid-feeding fishes. Frontiers in Ecology and Evolution 6: 22.

Costa, W.J.E.M. 1992. Description de huit nouvelles espèces du genre *Trichomycterus* (Siluriformes: Trichomycteridae), du Brésil oriental. Revue Française d'Aquariologie 18: 101–110.

Costa, W.J., E. Henschel, and A.M. Katz. 2020a. Multigene phylogeny reveals convergent evolution in small interstitial catfishes from the Amazon and Atlantic forests (Siluriformes: Trichomycteridae). Zoologica Scripta 49 (2): 159–173.

Costa, W.J., et al. 2020b. Historical review and redescription of three poorly known species of the catfish genus *Trichomycterus* from south-eastern Brazil (Siluriformes: Trichomycteridae). Journal of Natural History 53 (47–48): 2905–2928.

Dagosta, F.C.P., and M.C.C. de Pinna. 2021. Two new catfish species of typically Amazonian lineages in the Upper Rio Paraguay (Aspredinidae: Hoplomyzontinae and Trichomycteridae: Vandelliinae), with a biogeographic discussion. Papéis Avulsos de Zoologia 61: e20216147.

Datovo, A., and F.A. Bockmann. 2010. Dorsolateral head muscles of the catfish families Nematogenyidae and Trichomycteridae (Siluriformes: Loricarioidei): comparative anatomy and phylogenetic analysis. Neotropical Ichthyology 8: 193–246.

de Pinna, M.D., and F.C.P. Dagosta. 2022. A taxonomic review of the vampire catfish genus *Paracanthopoma* Giltay, 1935 (Siluriformes, Trichomycteridae), with descriptions of nine new species and a revised diagnosis of the genus. Papéis Avulsos de Zoologia 62.

de Pinna, M.C.C., and W. Wosiacki. 2003. Trichomycteridae (pencil or parasitic catfishes). *In* R.E. Reis, S.O. Kullander, and C.J. Ferraris (editors), Check list of the freshwater fishes of South and Central America: 270–290. Porto Alegre, Brazil: Editora da Pontifícia Universidade Católica do Rio Grande do Sul.

Devincenzi, G.J., and R. Vaz-Ferreira. 1939. Nota preliminar sobre un pygidido hematófago del Rio Uruguay. Archivos de la Sociedad de Biología de Montevideo 9(3): 165–178.

Di Caporiacco, L. 1935. Spedizione nello Beccari nella Guiana Britannica. Monitore Zoologico Italiano 46 (3): 55–70.

DoNascimiento, C. 2012. Sistemática y relaciones filogenéticas de la subfamilia de bagres parasitos Stegophilinae (Siluriformes: Trichomycteridae). Ph.D. dissertation, Universidad Central de Venezuela, Caracas, Venezuela.

DoNascimiento, C. 2015. Morphological evidence for the monophyly of the subfamily of parasitic catfishes Stegophilinae (Siluriformes, Trichomycteridae) and phylogenetic diagnoses of its genera. Copeia 103 (4): 933–960.

Eigenmann, C.H. 1917. Descriptions of sixteen new species of Pygidiidae. Proceedings of the American Philosophical Society 56: 690–703.

Eigenmann, C.H. 1918. The Pygidiidae, a family of South American catfishes. Memoirs of the Carnegie Museum 7: 259–398.

Fernández, L., and S.A. Schaefer. 2009. Relationships among the Neotropical Candirus (Trichomycteridae, Siluriformes) and the evolution of parasitism based on analysis of mitochondrial and nuclear gene sequences. Molecular Phylogenetics and Evolution 52 (2): 416–423.

Fricke, R., W.N. Eschmeyer, and R. Van der Laan. 2024. Eschmeyer's catalog of fishes: genera, species, references. Online resource (http: //researcharchive.calacademy.org/research/ichthyology/catalog/fishcatmain.asp), assessed 6 May 2024.

Giltay, L. 1935. Notes ichthyologiques. X – description d'une espèce nouvelle de Trichomycteridae. Bulletin du Musée Royal d'Histoire Naturelle de Belgique 11 (27): 1–3.

Henschel, E., A.M. Katz, and W.J. Costa 2021a. A new candiru of the genus Paracanthopoma (Siluriformes: Trichomycteridae) from the Araguaia River basin, central Brazil. Journal of Fish Biology 99 (6): 990–1997.

Henschel, E., M.J. Bernt, J.N. Baskin, R.E. Schmidt, and N.K. Lujan. 2021b. Osteology-focused redescription and description of the blood-feeding candirus *Paracanthopoma parva* and *Paravandellia alleynei* sp. n. (Trichomycteridae: Vandelliinae). Journal of Fish Biology 100 (1): 161–174.

Kelley, W.E., and J.W. Atz. 1964. A pygidiid catfish that can suck blood from goldfish. Copeia 1964 (4): 702–704.

Lundberg, J.G., and J.N. Baskin. 1969. The caudal skeleton of the catfishes, order Siluriformes. American Museum Novitates 2398: 1–49.

Machado, F.A., and I. Sazima. 1983. Comportamento alimentar do peixe hematófago *Branchioica bertonii* (Siluriformes, Trichomycteridae). Ciência E Cultura 35: 344–348.

Miles, C.W. 1943. Estudio economico y ecologico de los peces de agua dulce del Valle de Cauca. *In* Boletin Cientifico del Departamento del Valle de Cauca, Colombia: 1–99. Colombia, Cali: Instituto Valle Caucano de Investigaciones Científicas.

Miranda-Ribeiro, A. 1912. Loricariidae, Callichthyidae, Doradidae e Trichomycteridae. *In* Comissão de Linhas Telegraphicas Estrategicas de Matto-Grosso ao Amazonas: 1–31. Rio de Janeiro, Brazil: Comissão de Linhas Telegraphicas Estrategicas de Matto-Grosso ao Amazonas.

Miranda Ribeiro, A. 1918. Tres generos e dezesete especies novas de peixes Brasilieros. Revista do Museu Paulista 10: 631–646.

Ochoa, L.E., et al. 2017. Multilocus analysis of the catfish family Trichomycteridae (Teleostei: Ostariophysi: Siluriformes) supporting a monophyletic Trichomycterinae. Molecular Phylogenetics and Evolution 115: 71–81.

Ochoa, L.E., et al. 2020. Phylogenomic analysis of trichomycterid catfishes (Teleostei: Siluriformes) inferred from ultraconserved elements. Scientific Reports 10 (1): 2697.

Oyanedel, A., et al. 2018. Movement patterns and home range in *Diplomystes camposensis* (Siluriformes: Diplomystidae), an endemic and threatened species from Chile. Neotropical Ichthyology 16: e170134.

Roberts, T.R. 1972. Ecology of fishes in the Amazon and Congo basins. Bulletin of the Museum of Comparative Zoology 143 (2): 117–147.

Rodrigues, J.B. 1890. Poranduba amazonense: ou, Kochiyma-uara porandub. 1872–1887. G. Leuzinger.

Schmidt, R.E. 1993. Relationships and notes on the biology of *Paracanthopoma parva* (Pisces: Trichomycteridae). Ichthyological Exploration of Freshwaters 4 (2): 185–191.

Sereno, P.C. 2007. Logical basis for morphological characters in phylogenetics. Cladistics 23 (6): 565–587.

Taylor, W.R., and G.C. Van Dyke. 1985. Revised procedures for staining and clearing small fishes and other vertebrates for bone and cartilage study. Cybium 9: 107–109.

Zanata, A.M., and C. Primitivo. 2014. Natural history of *Copionodon pecten*, an endemic trichomycterid catfish from Chapada Diamantina in northeastern Brazil. Journal of Natural History 48 (3-4): 203–228.

Zuanon, J., and I. Sazima. 2005. Free meals on long-distance cruisers: the vampire fish rides giant catfishes in the Amazon. Biota Neotropica 5 (1): 109–114.

APPENDIX

Comparative Material

Paracanthopoma cangussu Henschel, Katz and Costa, 2021: UFRJ 12696, 1 (holotype), 11.8 mm SL; UFRJ 12183, 24 (paratypes), 10.6–13.9 mm SL; UFRJ 12243, 6 (paratypes) (cs), 11.3–11.9 mm SL; UFRJ 8518, 4 (paratypes) (cs), 15.7–15.2 mm SL: Brazil: Tocantins. *Paracanthopoma saci* Dagosta and de Pinna, 2021: UFRJ 11111, 38, 10.9–16.2 mm SL; UFRJ 11112, 5 (cs), 11.4–14.6 mm SL: Brazil: Mato Grosso do Sul. *Paracanthopoma* sp.: UFRO 22118, 39, 13–20 mm SL; Brazil: Rondônia: Ji-Paraná; INPA 33647, 6, 8.8–17.2 mm SL, Brazil: Amazonas: Novo Aripuanã; INPA 36875, 1, 30.9 mm SL; Brazil: Roraima: Caracaraí; INPA 494428, 1, 22.8 mm SL; Brazil; UFRJ 11111, 38, 10.9–16.2 mm SL; UFRJ 11112, 5 (cs), 11.4–14.6 mm SL; Brazil: Mato Grosso: Cáceres; AMNH 230907, 2, 17.0–19.0 mm SL; Venezuela: Amazonas. UFRJ 12696, 1, 11.8 mm SL, UFRJ 7697, 2, 11.9–13.0 mm SL; UFRJ 7698, 19, 8.6–9.8 mm SL; UFRJ 12183, 20, 10.6–13.9 mm SL; UFRJ 12243, 6 (cs) 11.3–11.9 mm SL; Brazil: Tocantins: Pium. UFRJ 8518, 4 ex. (cs), 15.7–15.2 mm SL; CICCAA 02694, 4, 8.0–10.0 mm SL; Brazil: Tocantins: Sandolândia. *Paravandellia oxyptera* Miranda-Ribeiro, 1917: USNM 296084, 1 (CT scan), ca. 20 m SL; Brazil: Rio Grande do Sul: Itaqui. MCP 42576, 1 (CT scan), 23.1 mm SL; Brazil: Goiás: Roselândia. MCP 23374, 1 (CT scan), 21.8 mm SL; Brazil: Paraná: Pinheirinho do Vale. *Paravandellia phaneronema* (Miles, 1943): MCZ 35874, 1 (X-ray), 25.3 mm SL; USNM 120141, 1 (X-ray), 28.1 mm SL; Colombia: La Virginia. ROM 112356, 1 (CT scan), ca. 20 mm SL; Colombia: Cauca River. *Paravandellia* sp.: UFRO 9548, 2, 22.0–25.0 mm SL; Brazil: Rondônia: Porto Velho; UFRO 9626, 12, 12.0–20.0 mm SL; Brazil: Rondônia: Porto Velho; INPA 48932, 1, 26.5 mm SL; Brazil: Amazonas: Japurá; INPA 37364, 3, 14.8–18.1 mm SL; Brazil: Roraima: Rorainópolis; INPA 39363, 14, 13–15.7 mm SL; Brazil: Roraima: Caracaraí; INPA 25121, 1, 22.6 mm SL, Brazil: Rondônia. *Vandellia cirrhosa* Valenciennes, 1846: UFRO 20619, 1, 106.0 mm SL; Brazil: Rondônia: Porto Velho; UFRO 9481, 15, 60.0–72.0 mm SL; Brazil: Rondônia: Manicoré; UFRO 984, 3, 70.0–73.0 mm SL; Brazil: Rondônia: Porto Velho.

All issues of *Novitates* and *Bulletin* are available on the web (https://digitallibrary.amnh.org/handle/2246/5). Order printed copies on the web from:
https://shop.amnh.org/books/scientific-publications.html

or via standard mail from:
American Museum of Natural History—Scientific Publications
Central Park West at 79th Street
New York, NY 10024

♾ This paper meets the requirements of ANSI/NISO Z39.48-1992 (permanence of paper).